Growth and shedding of captive harp seal (*Pagophilus groenlandicus*) vibrissae over one year

by

A thesis submitted to the School of Graduate Studies

in partial fulfilment of the requirements for the degree of

Master of Science

Department of Biology

Memorial University of Newfoundland

April 2024

St. John's   Newfoundland and Labrador

ABSTRACT

The harp seal (*Pagophilus groenlandicus*) is the most abundant marine mammal in the

Northwest Atlantic. Climate change negatively affects the sea ice that the species needs for

pupping and moulting, while also altering the composition and availability of the species' prey.

Analyzing vibrissae for biological and chemical markers can aid in understanding the overall

health, movements, and interactions of the animal with the environment. In this study, I

examined growth and shedding patterns of mystacial vibrissae using photogrammetry in three

captive harp seals over one year. I modelled vibrissa growth using von Bertalanffy growth curves

that followed an asymptotic growth profile. Shedding occurred in 24 out of 36 vibrissae across

the three seals in March and April, just before the moult of body pelage. Vibrissae grew for a

mean of 104 days (SD = 14.4), indicating a period of growth from late March until mid-July.

Vibrissa lengths varied greatly, so vibrissae in different positions could not be modelled using

the same von Bertalanffy parameter estimates. This research on harp seal vibrissa growth and

shedding will be helpful to future ecological and physiological studies including stable isotope

analysis, measuring reproductive and stress-related hormones, as well as the accumulation of

environmental pollutants.

DEDICATION

I dedicate this thesis to my family and colleagues in Newfoundland and Nova Scotia. To my family, thank you for the encouragement and support over the years. To Lincoln, Ophelia, and Fisher, thank you for inspiring me to be my best and offering me unwavering love and support.

ACKNOWLEDGEMENTS

TABLE OF CONTENTS

LIST OF TABLES

LIST OF FIGURES

LIST OF APPENDICES

LIST OF ABBREVIATIONS

cm/day - Centimeter per day

DDT - Dichlorodiphenyltrichloroethane

OSC - Ocean Sciences Centre

PCB - Polychlorinated biphenyls

POP - Persistent organic pollutants

PTFE - Polytetrafluoroethylene

Chapter 1 Introduction and overview

Harp seals

The harp seal, *Pagophilus groenlandicus*, is a migratory species that inhabits the eastern Canadian archipelago and western Greenland during the summer and fall, and subarctic areas of the Northwest Atlantic during the winter (Figure 1-1; Stenson & Sjare, 1997; Stenson et al., 2016). This species is the most abundant marine mammal in the North Atlantic and relies on sea ice for pupping, nursing young, and moulting (Stenson & Hammill, 2014). Harp seals leave the Arctic in the fall for three distinct breeding grounds: the Greenland Sea, the White Sea, and the Northwest Atlantic (Sergeant, 1965). The Northwest Atlantic population has two pupping areas: the Gulf of St. Lawrence and "the Front", which is off the northeastern coast of Newfoundland and southern Labrador (Figure 1-1; Sergeant, 1965; Stenson et al., 2003). Northwest Atlantic seals give birth on drifting pack ice from late February through late March (Sergeant, 1991). Male and juvenile harp seals begin their annual moult in early to mid-April, and females begin in late April (Sergeant, 1991). After moulting, adult and juvenile seals feed on the Newfoundland and Labrador shelf before commencing their northern migration (Figure 1-2; Stenson & Sjare, 1997). The migration timing is highly variable in both juveniles and adults (Stenson & Sjare, 1997; Grecian et al., 2022). Some adult seals migrate past the Northern Labrador Shelf in late June; others do not migrate until July or August, then eventually they reach the northern Canadian and Greenland continental shelves (Sergeant, 1991; Stenson & Sjare, 1997; Stenson et al., 2020).

Harp seals are vulnerable to climate change due to changes in sea ice, which is critical during specific periods of the year (e.g., for pupping and moulting). Reductions in ice thickness and coverage increases the risk of pup mortality, notably when the pups are nursing and learning to

dive, as storms can break the sea ice apart, and the pups can drown (Stenson & Hammill, 2014).

Climate change contributes to ecosystem changes that impact prey availability; this affects harp seal populations because common prey species have declined substantially over the past few decades (e.g., capelin *Mallotus villosus* and Atlantic cod *Gadus morhua*; Stenson et al., 2016). Pregnancy rates in harp seals are sensitive to interannual variations in environmental conditions, including capelin biomass and poor ice conditions (Stenson et al. 2016). High late-term abortion rates and low reproductive success occurred in years with low capelin abundance and poor ice conditions, including reduced ice coverage and thickness. Late-term abortions are related to female body condition, as females may abort the foetus if they have insufficient lipid stores to raise a pup to weaning without affecting their health (Stenson et al., 2020). The species' large range and extensive migration make it challenging to collect information on diet and life events throughout the annual cycle. However, vibrissae can be analyzed for specific biological and chemical markers to gain insight on ecological and physiological information the animal is experiencing, including foraging patterns, concentrations of reproductive and stress hormones, and environmental contaminants and pollutants.

Pinniped vibrissae

Pinnipeds have the largest and most developed vibrissae among mammals, which they use for tactile sensing, obstacle avoidance, social encounters, and hunting prey (Miller, 1975; Ling, 1977; Dehnhardt et al., 2001; Shatz & De Groot, 2013; Mattson & Marshall, 2016). Pinniped vibrissae have different surface structures, cross-sectional profiles, and orientations that influence how they interact with their environment (Ling, 1977; Marshall et al., 2006; Ginter et al., 2012; Hanke et al., 2013; Murphy, 2013). Most 'true' seals (Phocidae) have vibrissae with undulated surfaces, while otariids (eared seals) and odobenids (walrus) have vibrissae with

smooth surfaces (Murphy et al., 2013). Pinniped vibrissae are also highly innervated and provide haptic sensing capabilities, with ten times more nerve fibres than vibrissae in other mammals (Hyvarinen, 1989; Dehnhardt & Kaminski, 1995).

There are three kinds of vibrissae in phocids: rhinal vibrissae on top of the snout; supraorbital vibrissae above the eyes; and mystacial vibrissae on the upper lip (Figure 1-3; Ling, 1977; Bauer et al., 2018; Kruger et al., 2018). Rhinal and mystacial vibrissae have different functions; studies on supraorbital vibrissae are limited. Rhinal vibrissae alert the seal to open its nostrils when breaking the surface of the water or detecting sudden and unexpected movements, such as a fish suddenly changing direction (Yablokov & Klevezal, 1969; Smodlaka et al., 2017). Seals use their mystacial vibrissae to follow hydrodynamic trails created by prey, as well as haptic recognition of benthic prey in low-light environments encountered during dives below the photic zone (Dehnhardt et al., 2001; Kruger et al., 2018). Harbour seals (*Phoca vitulina*) can differentiate an object's size and shape from the pattern of the hydrodynamic trail and follow a hydrodynamic trail 40 meters behind a remote-operated submarine (Dehnhardt et al., 2001; Wieskotten et al. 2011). Mystacial vibrissae are also important during social encounters such as naso-nasal greetings between mothers and pups and interactions between dominant and subordinate seals (Miller, 1975; Miller & Kochnev, 2021).

Harp seals typically have 43-55 mystacial vibrissae distributed across eight to nine rows on each side of the face; vibrissae in the outer corners of the second and third rows have the thickest hair shafts, and the more medial vibrissae are finer (Figure 1-4; Yablokov & Klevezal, 1969; Mattson & Marshall, 2016). The number of vibrissae usually differs between the left and right sides and there is variability across individuals.

Mystacial vibrissae can be divided into fine short microvibrissae and large macrovibrissae

(Mattson & Marshall, 2016). Microvibrissae, located in columns 8 through 11, are densely

clustered around the snout, whereas macrovibrissae, in columns 1-7, are located more posteriorly

and are sturdier and longer (Figure 1-4; Dehnhardt, 1994; Mattson & Marshall, 2016). In harp

seals, these vibrissae are sensitive to different sound frequencies in air and water based on

length: shorter vibrissae respond to higher frequencies and longer vibrissae respond to lower

frequencies (Shatz & De Groot, 2013). Microvibrissae are used mainly for object recognition,

whereas macrovibrissae may be used for more spatial tasks such as detecting distance and

locating objects (Dehnhardt, 1994; Brecht et al., 1997; Dehnhardt et al., 2001; Mattson &

Marshall, 2016).

Ecological and physiological analyses of vibrissae

Stable isotope analysis

Stable isotopes are naturally occurring elements (e.g., C, N) that have different molecular

weights depending on the number of neutrons in the atom (Hobson & Wassenaar, 2008). The

ratios of the heavy to light forms of the isotope can be ecologically informative, including

foraging patterns and the trophic level of the consumer, whether an animal feeds on pelagic or

benthic prey, or in coastal or offshore environments (Hammill et al., 2005; Eglite et al., 2023;

Hobson, 2023). Stable isotope ratios in the tissues of an animal are correlated to their diet, and

enrichment of nitrogen-15 isotopes are predictable from one trophic level to the next, allowing

researchers to interpret the trophic level of the consumer (Minagawa & Wada, 1984; Hobson et

al., 1996; Lesage et al., 2001). The ratio of carbon-13 to carbon-12 relate to the source of

primary producers and are informative on whether the animal feeds in pelagic versus benthic

environments, and offshore versus nearshore areas (Ramsay & Hobson, 1991; Smith et al., 1996;

Page, 1997) Metabolization rates of stable isotopes differ among tissues and are metabolically

inert in keratinous tissues such as fingernails, hair, baleen, and vibrissae and are deposited

continuously as the tissue grows (Hobson et al., 1996).

The fractionation of isotopes between the diet, vibrissae, and other tissues have previously been studied in captive harp seals. Stable carbon and nitrogen isotope levels in the vibrissae of captive harp seals were +15.8 for nitrogen-15, and -17.1 for carbon-13 (Hobson et al., 1996). Mean fractionation values for a diet composed solely of herring were +2.8 for nitrogen-15 and +3.2 for carbon-13 (Hobson et al., 1996).

Stable isotope analysis has been used in many studies of marine mammals in captivity and the wild. These studies include the analysis of harp seal teeth to determine temporal changes in prey availability over multiple decades, in southern elephant seals (*Mirounga leonina*) to identify foraging strategies and their trophic ecology, and modelling vibrissa growth in a captive seal then applying their findings to identify life events in wild seals (Hobson et al., 1996; Huckstadt 2011; Beltran et al., 2016; De la Vega et al., 2023). Knowledge of vibrissa growth and shedding patterns can contribute to temporal interpretations of stable isotope patterns in terms of the seal's movements, and dietary preferences around the year.

Reproductive and stress-related hormones

Cortisol is released when an animal perceives a stressor and is related to many behavioural and physiological changes including fasting, moulting, and lactating (Ortiz et al., 2003; Kershaw & Hall, 2016). Concentrations of cortisol deposited in the vibrissa have been paired with stable isotope analysis to determine the relationship between diet and physiological status in ringed (*Pusa hispida*), spotted (*Phoca largha*), and harbour seals (Karpovich et al., 2019). While associations between cortisol concentrations and stable carbon and nitrogen isotopes were found, the researchers highlighted the need for fine-scale, species-specific growth profiles of the vibrissae to accurately interpret results.

5

Reproductive hormones including testosterone, progesterone and estradiol have been studied in many keratinous tissues including claw, baleen, and recently in vibrissae (Karpovich et al., 2020; Keogh et al., 2021; Lowe et al., 2021). All three reproductive hormones were measurable in the vibrissae, and cyclical patterns in progesterone, indicating pregnancies and luteal phases, were identified in the vibrissae of Steller sea lions (*Eumetopias jubatus*) and northern fur seals (*Callorhinus ursinus;* Keogh et al., 2021).

Mercury and other trace elements

Mercury is a global pollutant that affects the health and survival of animals and has been linked to neurological disorders, compromised reproduction and embryonic development (Driscoll et al., 2013; Rea et al., 2020). Mercury can bio-magnify through marine food webs and bio-accumulate in animal tissues over time (Rea et al., 2019; Gastaldi et al., 2023). Recent studies on pinniped vibrissae have paired stable isotope analysis with mercury concentrations to understand seasonal and long-term changes in mercury concentrations in free-ranging, migratory animals (Rea et al., 2019; Kooyomjian et al., 2022; Gastaldi et al., 2023).

Concentrations of other trace elements including arsenic and lead can also be measured through vibrissa analysis to determine how environmental contaminants are affecting animal populations (Kooyomjinan et al., 2022). Arsenic is a known carcinogen and can cause cardiovascular and neurological disorders, while long term exposure to lead can lead to kidney and brain damage (von Ehrenstein et al., 2006; Jaishankar et al., 2014). Concentrations of trace elements have been paired with stable isotope analyses of the vibrissae of Peruvian fur seals (*Arctocephalus australis*) and South American sea lions (*Otaria byronia*) to compare differences in years of El Niño to La Niña (Kooyomjinan et al., 2022).

Persistent organic pollutants

Persistent organic pollutants (POPs) consist of pesticides, industrial chemicals and by-products of industrial processes that do not readily degrade in nature (Dauwe et al., 2004; Alharbi et al., 2018). These pollutants can bio-accumulate in tissue and cause health problems including impaired fertility, cancer, and physical abnormalities (Alharbi et al., 2018). Recently, researchers have used feathers of the great tit (*Parus major*) to study POP concentrations including polychlorinated biphenyls (PCBs) and dichlorodiphenyltrichloroethane (DDT) (Dauwe et al., 2004). Concentrations of POPs have not yet been measured in vibrissae, however based on the success in feathers, further research is warranted.

Methods for measuring vibrissa growth

Many methods have been used to study vibrissa growth, including clipping vibrissae flush with the face, and measuring regrowth over time; isotope tracers incorporated into the diet; and photogrammetry, where the vibrissae are repeatedly photographed and then measured digitally (Hirons et al., 2001; Beltran et al., 2015; Lübcker et al., 2016). Vibrissae of tagged free-ranging southern elephant seals were measured by clipping the vibrissae flush with the face, measuring regrowth, and observing shedding patterns (Lübcker et al., 2016). Captive harbour seals and Steller sea lions were administered ^{13}C- and ^{15}N- labelled glycine at two times and vibrissa growth was calculated between the two isotopic markers (Hirons et al., 2001). Lastly, photogrammetry is a non-invasive way to document vibrissa growth. The vibrissae of a captive northern elephant seal (*Mirounga angustirostris*) were measured by repeatedly photographing the vibrissae of the seal with a scale bar visible in the frame. The vibrissae lengths from the photographs were measured digitally, and growth rates were calculated based on changes in length over time (Beltran et al., 2015). Photogrammetry was also used to investigate vibrissa growth in captive California sea lions (*Zalophus californianus*), spotted seals (*Phoca largha*),

northern elephant seals, a ringed seal (*Pusa hispida*), a bearded seal (*Erignathus barbatus*), and a Hawaiian monk seal (*Neomonachus schauinslandi*) by photographing vibrissae over variable periods ranging from months to years then measuring the lengths digitally (McHuron et al., 2016, 2018, 2020).

The last method, photogrammetry, requires minimal scientific equipment and specialized training. In addition, captive seals can be photographed repeatedly and in uniform conditions, yielding accurate and consistent measurements. In this study, I used photogrammetry on captive harp seals over an entire year to measure vibrissa growth and to observe patterns in vibrissa shedding and lifespan. The objective of my research was to measure and model the growth and lifespan of harp seal macrovibrissae. This information will help us understand the timing of vibrissa growth and shedding, that can enhance temporal aspects of ecological and physiological studies on the vibrissae of this species. There is no published literature on vibrissa growth rates, longevity, or shedding in harp seals, and this information will be useful to researchers who are interested in using vibrissae for analyses.
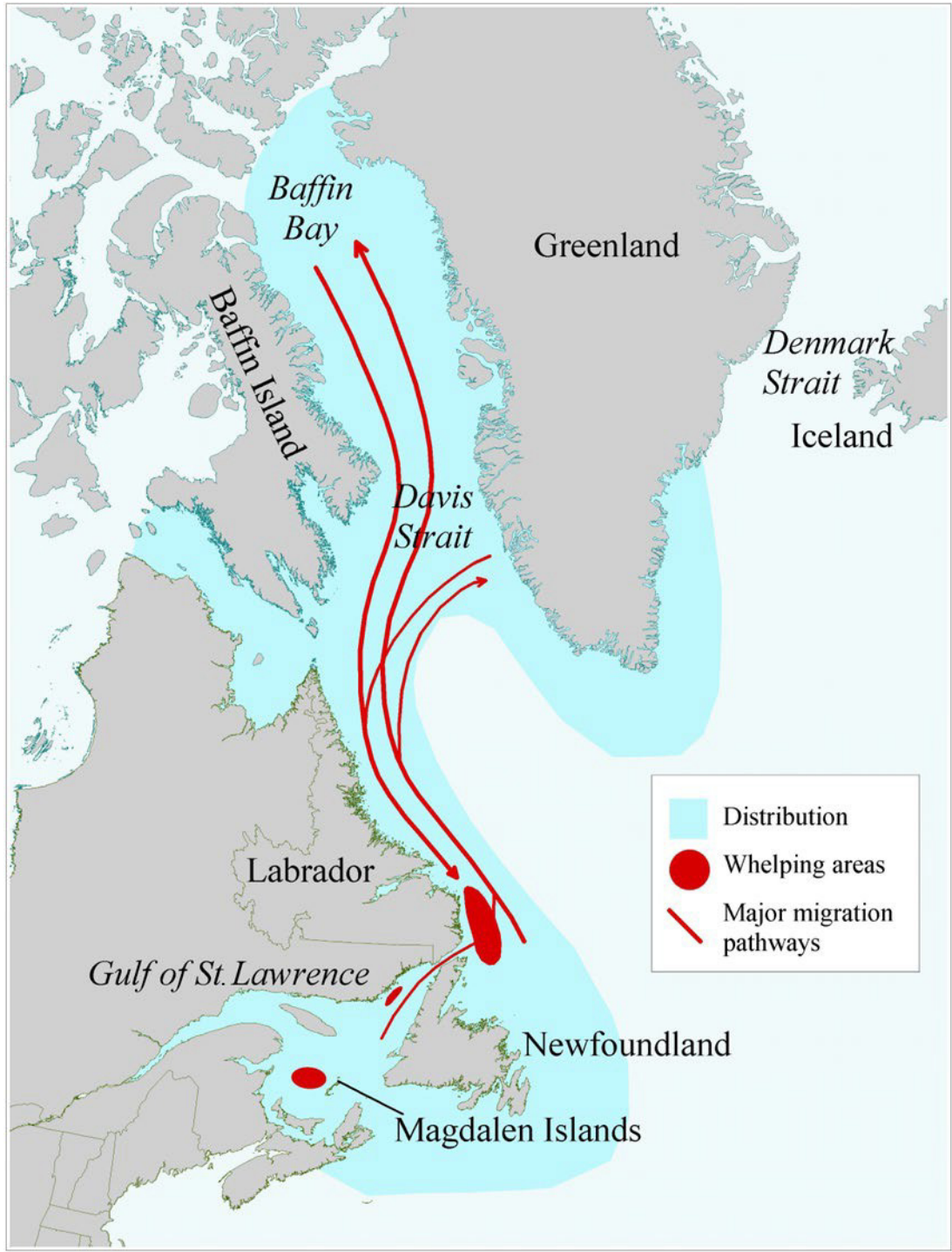
Figure 1-1. Seasonal distribution of northwest Atlantic harp seals adapted from Stenson et al. (2016).
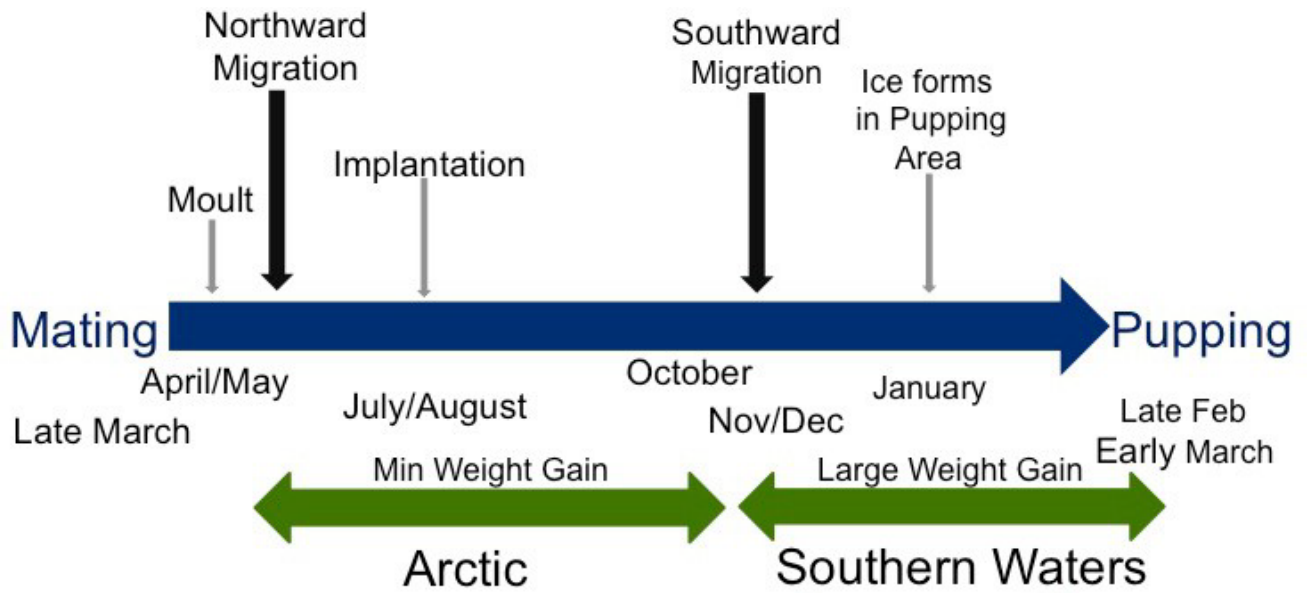
Figure 1-2. Annual cycle of pregnancy, movements, and weight gain in northwest

Atlantic harp seals adapted from Stenson et al. (2016).
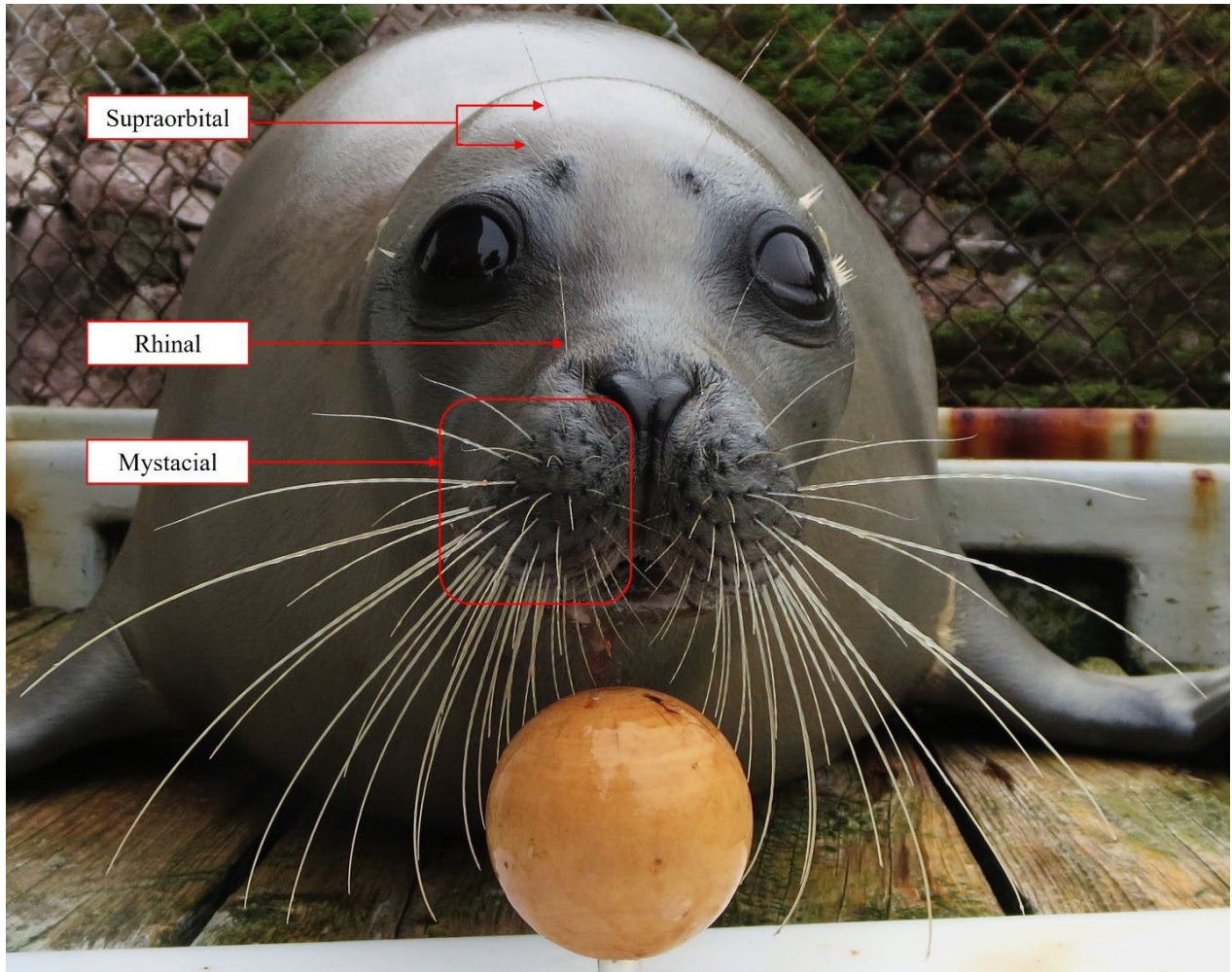
Figure 1-3. Phocid seals have three types of vibrissae: supraorbital, above the eyes; rhinal, behind the nostrils; and mystacial, on the upper lip.
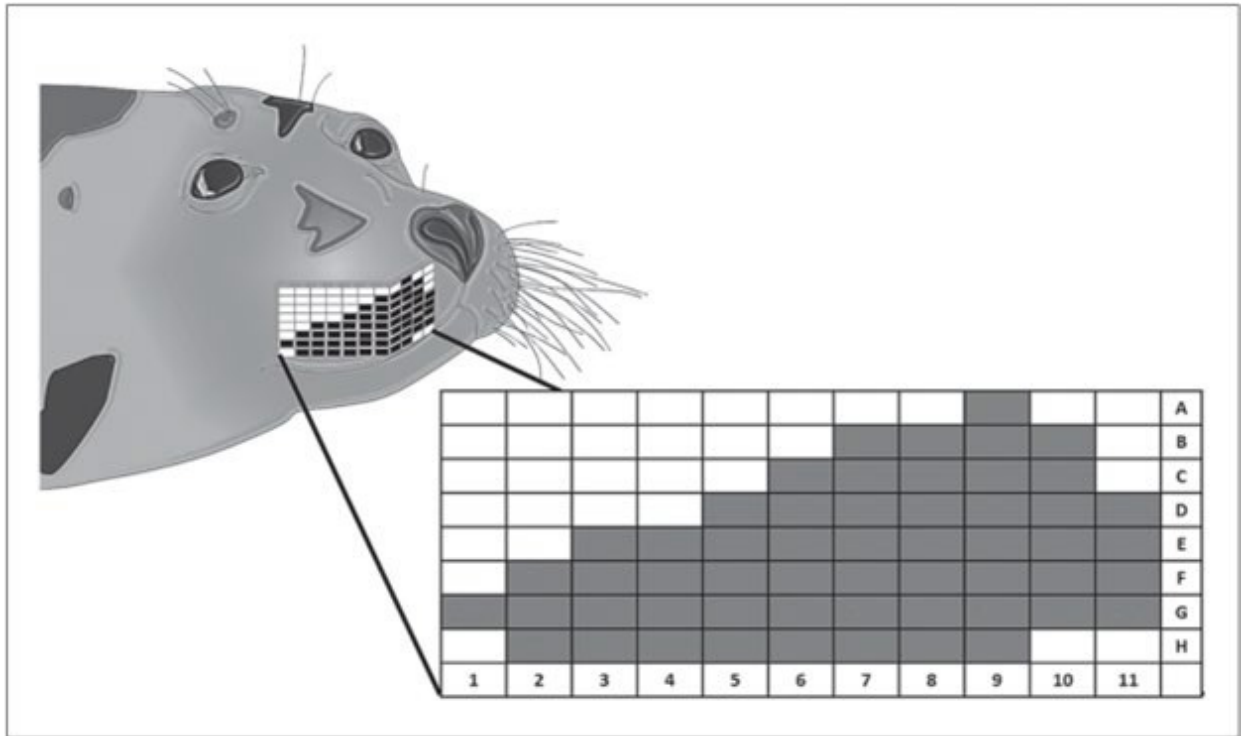
Figure 1-4. Standardized distribution of vibrissae into rows and columns for harp seals (*Pagophilus groenlandicus;* adapted from Mattson & Marshall (2016). Shaded cells represent vibrissa positions; columns 1 through 7 are macrovibrissae; columns 8 through 11 represent microvibrissae.

Chapter 2 Growth dynamics and shedding patterns of harp seal vibrissae

2.1 Introduction

Knowledge of species-specific vibrissa growth rates is needed for studies on pinniped vibrissae because species differ in patterns of growth and shedding (Greaves et al., 2004; Beltran et al., 2015; Lübcker et al., 2016; McHuron et al., 2016; McHuron et al., 2018; McHuron et al., 2020; Karpovich et al., 2022). Otariids generally exhibit linear vibrissa growth, whereas phocids have non-linear or irregular growth (McHuron et al., 2016). For instance, vibrissae grow to an asymptotic length in southern elephant seals (*Mirounga leonina*), northern elephant seals (*Mirounga angustirostris*), spotted seals (*Phoca largha*), and harbour seals (*Phoca vitulina*; Hirons et al., 2001; Beltran et al., 2015; Lübcker et al., 2016; McHuron et al., 2016). Spotted seal vibrissae reached 95% of their asymptotic length in 105 days, whereas harbour seal vibrissae took approximately 240 days to reach asymptotic lengths (Hirons et al., 2001; McHuron et al., 2016). Vibrissae of otariids including California sea lions (*Zalophus californianus*), Steller sea lions (*Eumetopias jubatus*), and Antarctic fur seals (*Arctocephalus gazella*) exhibit linear growth that never reaches an asymptote (Kernaléguen et al., 2012; Rea et al., 2015; McHuron et al., 2016). Hawaiian monk seals (*Neomonachus schauinslandi*) and bearded seals (*Erignathus barbatus*) have a unique growth pattern for phocids, characterized by rapid growth of the new vibrissa after shedding of the old, that slows and grows linearly until the next shedding event, which may be related to the vibrissae being constantly abraded by their benthic foraging patterns (McHuron et al., 2020).

Vibrissa lifespan and shedding also differ across otariids and phocids. Captive spotted seals shed over half of their vibrissae during their annual pelage moult (McHuron et al., 2016). In contrast, captive California sea lions do not shed their vibrissae annually and have a vibrissa lifespan of over

ten years (McHuron et al., 2016). Therefore, when analyzing the vibrissae for temporal biomarkers, it is important to understand the period of vibrissa growth and retention to properly interpret the results.

There have been numerous ecological and physiological analyses on otariid vibrissae where the predictable linear growth of the vibrissae is easy to interpret (Keogh et al., 2021; Gastaldi et al., 2022; Kooyomjian et al., 2022). When studying phocids, the period of asymptotic vibrissa growth and retention differs by species, making the interpretation of vibrissa growth analyses challenging (Beltran et al., 2015; McHuron et al., 2018; Karpovich et al., 2019). Researchers have highlighted the need for fine-scale, species-specific vibrissa growth profiles to accurately interpret the results of ecological and physiological studies of vibrissae (Karpovich et al., 2019).

This study aimed to characterize vibrissa growth in harp seals using linear, or non-linear equations and to determine whether von Bertalanffy equations could be uniformly applied across vibrissae positions and between seals. Based on trends in other phocid species, I predicted that: (1) vibrissae would grow to an asymptotic length; (2) vibrissae would be shed annually, synchronous with the annual moult of body pelage; (3) growth could be modelled using von Bertalanffy equations; and (4) vibrissa length would limit the ability to use the same von Bertalanffy parameter estimates to model all vibrissae.

2.2 Methods

2.2.1 Seals

The study subjects were three captive harp seals, *Babette, Tyler*, and *Deane*, housed in an outdoor facility at the Department of Ocean Sciences (OSC) in Logy Bay, Newfoundland and Labrador, Canada (47.62° N, 52.66° W). The seal enclosure consisted of two circular tanks with a depth of 2.5 m and diameters of 7.5 and 4.9 m, plus a rectangular tank with dimensions 3.8 x 1 m across and a depth of 1.3 m. Each tank had flow through ambient seawater at a rate of 5-6 litres per second. Wooden decking surrounded the tanks, and the seals were free to haul out

among the tanks.

Two of the seals were originally caught in the wild while one seal was born at the facility. *Babette* (female) was captured off the Magdalen Islands, Quebec, Canada (47.38° N, 61.88° W) in 1989 as an adult; *Tyler* (male) was captured near the Magdalen Islands, Quebec, Canada, as a whitecoat (newborn) in 1990; and *Deane* (female) is an offspring of *Babette* and *Tyler*, born at the facility in 2004. The seals were fed a diet of Atlantic herring (*Clupea harengus*) and capelin (*Mallotus villosus*) with a daily multivitamin and cysteine supplement. They had a constant supply of freshwater ice for consumption. The seals were weighed weekly using a hanging scale attached to a large cage. The body condition of the seals followed a seasonal pattern, where the seals were at their lowest body mass at the end of May and beginning of June, then reached their highest mass in January and February (Figure 2-1). The overall trend in body condition was consistent with wild harp seals that reach their highest body mass by February, then rapidly lose mass while fasting during whelping and moulting, to reach a minimum by May (Chabot et al., 1996). The feeding regimen of wild seals was mimicked by the captive seals during the moulting period; daily herring allotments were reduced, and the seals often refused feedings.

2.2.2 Vibrissa photography station

The vibrissa photography station was constructed from a polytetrafluoroethylene (PTFE) base, with a round wooden knob used as a target that was positioned at a fixed distance, height, and angle from the camera. A centimeter scale bar was attached directly below the target and angled in the same direction as the vibrissae (Figure 2-2). I trained the seals to rest with their chin on the wooden target while twenty photographs were taken; ten photographs of the vibrissae on each of the left and right sides of the face were captured (Figure 2-3). As positive reinforcement, the seals were rewarded with a piece of herring after each photograph. The seals participated willingly and were never forced to participate in the photography sessions.

Photographs were taken using a Canon PowerShot ELPH, 20-megapixel camera, and during each sampling event, three photographs of the left and right of each seal's face were selected for analysis. Criteria for analysis included visual clarity, visible whisker follicle, and the entire vibrissa being visible in the photograph. The photography sessions were conducted weekly from 5 April 2017 to 4 April 2018.

2.2.3 Data analysis

2.2.3.1 Selection of vibrissae for analysis

I identified vibrissae based on a standardized alphanumeric diagram of vibrissae arranged into rows and columns, developed by Sadou et al. (2014), that was modified for harp seals by a previous staff member at the OSC (Figure 2-4). Micro- and macrovibrissae were labelled on the standardized alphanumeric diagram based on Mattson and Marshall (2016). I chose the two exterior macrovibrissae in rows A, B, and C for analysis since they were consistently identifiable in the photographs and were not obscured from view. Each vibrissa position was given a unique identification code based on the seal, the side of the face, and the position. For example, *Babette*'s left vibrissa in row A, position two, was identified as BLA2.

2.2.3.2 Plotting vibrissa growth and shedding

I measured vibrissa lengths using Image Processing and Analysis in Java (ImageJ) software (Schneider et al., 2012), by calibrating the measurement tool to the centimeter scale bar in the photograph. This calibration used the Analyze function in ImageJ and Set Scale to one centimeter, with a separate calibration performed for each image (Figure 2-5). I measured the vibrissae using the segmented line tool to follow the natural curve of the vibrissa. Triplicate vibrissa length measurements were recorded for each sampling event using three photographs from each side of the seal's face. If none of the photographs met the criteria for analysis for a

sampling event, that event was excluded.

I used triplicate vibrissa lengths from the three photographs when plotting data to better visualize the measurement precision. The coefficient of variation was calculated for individual vibrissae on each sampling event; then I calculated mean percentages of the coefficient of variation for each vibrissa position, row, and seal.

The maximal growth rate for each vibrissa was calculated as the change in mean vibrissa length from each sampling event divided by the number of days between successive sampling events. Vibrissa shedding was documented during the photography sessions based on the presence or absence of a vibrissa in each of the twelve positions. Lifespan was calculated as the difference between the dates when each vibrissa first appeared and was shed. The accuracy of estimates was affected by the 1-week interval between successive photographs. Lifespans could not be calculated if a vibrissa was not shed by the end of the study or if it had shed and began to regrow before the study began.

2.2.4 Modelling vibrissa growth

The growth of each vibrissa was modelled using a von Bertalanffy growth equation:

$$L_t = L_\infty \cdot (1-e^{-k(T-T_o)}),$$

L_t = length at time (T)

L_∞ = asymptotic length of the vibrissa

K = a curvature constant that predicts the length of the vibrissa at time (T)

T_o = date of first appearance.

Vibrissa lengths for each seal were sorted by vibrissa position, and the data were trimmed to include only the new growth cycle. Therefore, the day the vibrissa first appeared was

considered Day 1 for von Bertalanffy modelling. If a vibrissa shed and new growth commenced before the start of the study, a negative T_o value would be calculated to estimate the initial time of growth.

I estimated growth model parameters using Ford-Walford plots, then adjusted the estimates using a least-squares von Bertalanffy fit function in RStudio software (v4.3.0; R Core Team, 2021; Cubillos, 2021). Parameter estimates were calculated for twelve vibrissae of each seal. I then compared the growth of the left and right vibrissae using linear regression and listed the coefficient of correlation in each plot.

I calculated the breakpoint for each of the vibrissae above using the BreakPoints package in RStudio. The breakpoint in the vibrissa length data indicates when the vibrissae reached their respective asymptotic lengths, and stopped growing (Hurtado et al., 2020; v4.3.0; R Core Team, 2021). The BreakPoints function used a Pettitt test that detects a shift in the central tendency of the data (Pettitt, 1979). Two hypotheses were tested at a significance level of $\alpha = 0.05$; the null hypothesis that states there is no change in the central tendency of continuous data, and the alternative hypothesis states there is change (Pettitt, 1979).

2.2.5 Comparison of vibrissa growth within and across seals

I used a growth-likelihood ratio test to compare the parameter estimates of the von Bertalanffy equations (Cerrato, 1990). Likelihood-ratio tests use a series of null and alternative hypotheses for each parameter to compare estimates, where the null hypothesis states that estimates of a parameter are equal (Cerrato, 1990). Four alternative hypotheses were compared to the null, one for each parameter of the von Bertalanffy equations and a combination of all parameters (Appendix A).

I computed the likelihood-ratio tests using the growth likelihood-ratio function in the

fishmethods package in RStudio (Kimura, 1980; Nelson, 2021; R Core Team, 2021). I used

trimmed data and von Bertalanffy parameter estimates from Section 2.2.4 for this analysis.

Asymptotic lengths of the vibrissae differed significantly across rows, so only vibrissae in the

same alphanumeric position were compared. For all tests, a significance level of $\alpha = 0.05$ was

selected. Two series of likelihood-ratio tests were completed to compare the vibrissae within and

across seals.

Within-seal comparison

The first series of likelihood-ratio tests tested whether vibrissae in a specified

alphanumeric position differed in von Bertalanffy parameter estimates on the left and right sides

of the seal's face. The assumption that the left and right vibrissae in the same position will grow

to similar asymptotic lengths has been made in previous studies (e.g., northern elephant seals;

McHuron et al., 2018). Tests were completed for the six (6) left and right pairs of vibrissa

positions for each seal. Based on the calculated p-value of the likelihood-ratio test, I decided

whether to reject the null hypothesis at the $\alpha = 0.05$ significance level, thus deciding if the

parameter estimates of the von Bertalanffy equation differed for each vibrissa position on the

left and right.

Across-seal comparison

The next series of likelihood-ratio tests were designed to compare vibrissae in the same

alphanumeric position across the three seals. Asymptotic lengths, growth constants, and the time

of initial growth were tested to determine whether vibrissae in the same alphanumeric position

differed across seals. For this series of tests, the left and right sides were combined. This

comparison resulted in six likelihood-ratio tests, one for each alphanumeric pair of vibrissae.

Parameter estimates were considered different if the null hypothesis, stating that parameter

estimates are equal, was rejected at the $\alpha = 0.05$ significance level, represented by a p- value of

less than 0.05.

The results of these likelihood ratio tests determined whether von Bertalanffy parameter estimates can be shared to model vibrissae across alphanumeric positions and seals. von Bertalanffy equations help estimate the age of vibrissae in free-ranging seals, which is crucial for temporal applications of biomarker studies. Therefore, knowing whether parameter estimates can be shared to model vibrissae across seals or alphanumeric positions is necessary for ecological and physiological vibrissa studies.

2.3 Results

2.3.1 Vibrissa growth

Over the study period, I measured 4758 vibrissa lengths across the three seals. Vibrissa growth followed a non-linear pattern characterized by rapid initial growth that slowed as the vibrissa approached an asymptotic length (Figures 2-6A – 2-6I). Breakpoint analysis indicated the mean vibrissa growth period across positions was 104 days (SD= 14.4; Table 2-1; Figures 2-7A – 2-7I). Breakpoints for the vibrissae ranged from 78 to 127 days after shedding, suggesting the vibrissae stopped growing between 22 June 2017 and 18 August 2017. The C1 position had the longest mean growth period at 116 days and position A3 had the shortest growth with a mean of 90 days (Table 2-1). The change in length for the remainder of the year was near- zero or negative, likely from breakage and abrasion at the vibrissa's tip. The timing of vibrissa regrowth was closely correlated with pelage moult; moulting started on 11 April for *Babette* and 19 April for *Tyler* and *Deane.* Maximal growth rates ranged from 0.14 cm/day to 0.47 cm/day, and mean growth rates over the whole study period ranging from 0.0003 to 0.0040 cm/day (Table 2-2).

Measurements of vibrissa length from individual sampling events often varied substantially due to errors inherent to the photogrammetric method (see Section 2.4). The overall coefficient of variation for vibrissa length measurements was 6.1% and ranged from 4.5 – 9.3% across vibrissa positions (Table 2-3). I could not record vibrissa measurements in several sampling sessions. *Babette* refused to participate on 18 August 2017 and 1 February 2018. Deane refused to participate on 10 May 2017 and 4 April 2018. Photographs of *Deane*'s RC2 vibrissa were not always clear, and therefore, there were no measurements for the following dates: 11 April 2017, 10 May 2017, 30 August 2017, 18 January 2018, and 25 January 2018. Photo clarity was poor for the LC1 vibrissa, and no photographs met the analysis criteria on 5 October 2017, 16 October 2017, 22 November 2017, 13 December 2017, 1 February 2018, 20 February 2018, and 5 March 2018.

2.3.2 Shedding and vibrissa lifespan

Prior to the commencement of the study on 5 April 2017, 19 of the 36 vibrissae had already shed (Table 2-4). *Babette* shed her vibrissae earlier than *Deane* and *Tyler*, with nine of her vibrissae shed before 5 April 2017, and the remaining three between 6 April and 11 April 2017. *Tyler* shed his vibrissae later than *Babette* and *Deane*, with 10 of 12 vibrissae shed between 5 April 2017 and 19 April 2017 (Tables 2-4 and 2-5). A second shedding event was recorded from 5 March to 4 April 2018. The highest number of vibrissae shed was from 5 March to 27 March 2018, when 16 of 36 vibrissae were shed across the three seals (Table 2-5). I did not photograph the right side of *Deane*'s face on the last sampling event, 4 April 2018, so I could not calculate lifespan and shedding for five of her vibrissae. Seven of *Tyler*'s vibrissae did not shed by the end of the study. However, in the previous year, his vibrissae shed later in April; therefore, the observation was expected. Vibrissa lifespans ranged from 349 to greater than 364 days (Table 2-4).

2.3.3 Modelling vibrissa growth

I fitted von Bertalanffy growth models to the thirty-six vibrissae (Figures 2-7A – 2-7I). Parameter estimates for the growth constant K, asymptotic lengths, and time of initial growth are summarized in Table 2-6. Based on asymptotic lengths, vibrissae in row B were usually the longest, and vibrissae in the most posterior positions were longer than those in more medial positions in all three rows (Table 2-7). *Deane* and *Tyler* each had three of the longest vibrissae, while *Babette* most often had the shortest (Tables 2-6 and 2-7). *Tyler*'s left A2 vibrissa was much shorter than on the right side (Figure 2-7D). There were no discernable patterns in K growth coefficients or estimates for the initial time of growth across seals, rows, or vibrissa positions (Table 2-6).

2.3.4 Within-seal model comparison

I completed likelihood-ratio tests to compare von Bertalanffy parameter estimates for vibrissae in the left and right positions of each seal's face. A summary of the p-values from each likelihood-ratio test is available in Table 2-8.

Babette

There was no difference in parameter estimates for *Babette*'s B2 position (Table 2-8; Figure 2-8A). Her B2 and C1 vibrissae had no difference in asymptotic length estimates on the left and right sides, and only C1 had different K growth constant estimates. Estimates for the initial time of growth were equal in each of the left and right pairs (Table 2-8).

Tyler

There was no difference in parameter estimates for *Tyler*'s growth constant K in left and right pairs in five (5) of six (6) vibrissa positions, and estimates for initial time of growth were equal in four (4) of six (6) left and right positions (Table 2-10). All estimates of asymptotic lengths differed; therefore, full von Bertalanffy equations differed for all vibrissa pairs (Table 2-

8; Figure 2-8B).

Deane

Four (4) of six (6) of the full von Bertalanffy equations could be shared on the left and right sides (Table 2-10; Figure 2-8C). Asymptotic lengths differed in two left and right pairs, and B1 was the only vibrissa pair with different estimates of growth constant K. Estimates for the initial time of growth were comparable in all left and right vibrissa pairs (Table 2-8).

2.3.5 Across-seal model comparison

When comparing vibrissa positions across seals, all von Bertalanffy models and estimates of asymptotic length were different (Table 2-9; Figure 2-9). Two vibrissa positions had similar estimates for growth constant K and estimates for the initial time of growth.

2.4 Discussion

This study aimed to characterize vibrissae growth in harp seals using linear, or non-linear equations and to determine whether von Bertalanffy equations could be uniformly applied across vibrissae positions and between seals. Based on trends in other phocid species, I predicted that: (1) vibrissae would grow to an asymptotic length; (2) vibrissae would be shed annually, synchronous with the annual moult of body pelage; (3) growth could be modelled using von Bertalanffy equations; and (4) vibrissa length would limit the ability to use the same von Bertalanffy parameter estimates to model all vibrissae.

Characterization of harp seal vibrissa growth

The vibrissae grew to asymptotic lengths. Overall, the mean period of vibrissa growth was 104 days (SD = 14.4), which corresponded to mid-July. Some vibrissa lengths decreased after reaching an asymptote, suggesting breakage or wear of the tip. The pattern of rapid growth after

23

shedding, followed by slow growth to an asymptotic length, has been noted in most other studies on phocids (Greaves et al., 2004; Liying & Schell, 2004; Lübcker et al., 2016; McHuron et al., 2016; McHuron et al., 2020; Karpovich et al., 2022). Exceptions to this growth profile in phocids include the Hawaiian monk and bearded seals (McHuron et al., 2020). Vibrissae in those species have rapid linear growth post-shedding, followed by slow linear growth until the next shedding event, which did not have a temporal pattern or relation to the pelage moult (McHuron et al., 2020). This growth pattern could be attributed to the foraging behaviour of the monk and bearded seals; the vibrissae need to constantly regrow due to abrasion and breakage of vibrissa tips while searching for prey in benthic sediments (Wilson et al., 2017; McHuron et al. 2020).

Harp seal vibrissa shedding

Vibrissa shedding followed a temporal pattern for the captive harp seals in this study, occurring just prior to the annual pelage moult in April through May. Although only twelve vibrissa positions were documented in the current study, most of the mystacial vibrissae appeared to be shed synchronously. However, a complete profile of shedding would warrant further study. Vibrissa shedding has been documented in other pinniped species, and its timing is species-specific (Table 2-10). *Babette* and *Deane* started their shedding cycles before *Tyler*, contrasting with Sergeant (1991), who noted that male and juvenile harp seals moult in early April and adult females that are reproductively active, in late April. However, neither of the females in this study were bearing pups or nursing and, therefore, would not have reason to delay moulting. Temporal shedding patterns have been described for ringed, spotted, southern elephant, and harbour seals. Hawaiian monk seals, grey seals (*Halichoerus grypus*), and bearded seals shed their vibrissae sporadically and do not show any temporal trends (Table 2-10). Otariids, including the California sea lion, do not shed their vibrissae annually, and many have vibrissa lifespans of multiple years

(McHuron et al., 2016).

Regrowth of the vibrissae began in late March to early May, at the same time as the annual pelage moult, which started in mid-April and lasted approximately four weeks. Harp seals haul out onto the ice during the moult and limit feeding, resulting in a substantial loss in body mass and heavy reliance on stored lipids for energy (Chabot et al., 1996). Mystacial vibrissae that are shed synchronously with the moult would limit the ability of the seal to search for food. However, by timing the shedding with the haul out period, the seal can replace their vibrissae during a time when feeding is minimal (Beltran et al., 2015).

Modelling vibrissa growth using linear or non-linear equations

von Bertalanffy equations have been used in previous studies to model phocid vibrissa growth (Greaves et al., 2004; Beltran et al., 2015; McHuron et al., 2016; McHuron et al., 2020; Karpovich et al., 2022). The estimates of growth coefficient, K, for all vibrissae, were consistent with values observed in harbour seals, spotted seals, grey seals, ringed seals, and a captive northern elephant seal (Table 2-10). The asymptotic lengths of the vibrissae varied in relation to their position, as observed in other phocids. Vibrissa growth rates and lengths were similar within each seal but differed across seals. When comparing the left and right sides of the same vibrissa in 18 pairs, 15 pairs had the same K growth coefficient and initial time of growth. However, when comparing the same vibrissa position across the three seals, only one-third of the K growth coefficients were the same. All vibrissa lengths were different across seals. Therefore, individual von Bertalanffy models for vibrissa growth are not just species-specific for harp seals but are unique to the individual seal.

Measurement accuracy

Photogrammetry is a common method to measure anatomical lengths in living animals; however, measurement accuracy can be affected by several sources and needs to be controlled through experimental design. Controls for measurement accuracy include standardizing the position of the animal (Bell et al., 1997) with fixed camera angles, heights, and distances to the target, as well as validating measurements from photogrammetry with direct measurements from the live animal (Sadou et al., 2014).

The accuracy of measurements within a sampling event can be harder to control through experimental design, resulting in measurement length variations. These variations occur due to animal behaviour and the analysis of curved three-dimensional objects in two-dimensional photographs (Kelley et al., 1973). Variations in vibrissa measurements arose in this experiment from the vibrissae not being directly perpendicular to the camera, the position of the seal's chin on the wooden target, and the scale bar shifting in either direction in high wind conditions. I tried to control for variation by analyzing triplicate vibrissa lengths for each sampling event. Variations in measured lengths of vibrissae within individual sampling sessions are illustrated in Figures 2-6A – 2-6I and the overall mean coefficient of variation across positions and seals was 6.1%.

A calibration procedure was established to compare photogrammetry measurements to those taken directly from the vibrissa (Sadou et al., 2014). When proper controls were established to standardize the experimental design, measurement accuracy in the photogrammetric method was reliable to within ± 1 mm of the direct animal measurements (Sadou et al., 2014). Unfortunately, due to the behaviour of the seals in this study, I could not take direct vibrissa measurements or complete a calibration procedure to estimate measurement accuracy.

Implications for future ecological and physiological studies on vibrissae

The short period of vibrissa growth has implications for ecological information that can be gained from biological and chemical markers stored in the vibrissae. The vibrissa tissue would grow for approximately 104 days or until mid-July, and mid-August for the slowest growing vibrissae. Life events during this period include moulting, feeding prior to migration, the northern migration, and Arctic inhabitation. It is possible that reproductive and stress hormones from mating in late March and implantation in July or August could also be measured in the tissue of the vibrissa.

The moulting period is characterized by enriched nitrogen-15 isotopes in the tissue due to fasting and the metabolization of stored lipids (Beltran et al., 2015; Doi et al., 2017). When analyzing the vibrissae for stable isotopes, the change from high to low nitrogen-15 isotope levels could indicate when the moult is finished, and the period directly after the moult would be informative on where the seals are feeding, and the prey they are consuming. Generally, both Canadian subpopulations of harp seals migrate to the subarctic feeding grounds following the moult, but the timing varies (Sergeant, 1965; Stenson & Sjare, 1997). Before migrating north, many seals feed for up to a month on the Newfoundland and Labrador shelf (Stenson & Sjare, 1997). Some seals migrate to the Northern Labrador Shelf in late June, while others do not migrate until July or August (Stenson & Sjare, 1997). However, the ratios of carbon-13 and nitrogen-15 isotopes could be informative on the timing of the migration due to changes in distinct isotopic compositions across isoscapes identified in the North Atlantic (Espinasse et al., 2022).

Estimating the age of a vibrissa for future ecological and physiological analyses will be challenging since the same parameter estimates cannot be shared across seals. This is highlighted

in Figure 2-10, where a vibrissa of age 50 days could range in length from approximately 3 to 8 cm based on vibrissa position. Likewise, a vibrissa that is 5 centimeters long could range in age from 20 to 120 days (Figure 2-10). Therefore, it will be challenging to correctly age a vibrissa based on the length as there is high individual variability. However, knowing that the period of growth is approximately 100 days, and that the vibrissae are shed synchronously just prior to the moult, provides valuable information for future studies. It is worth noting that individual timing of the moult may vary across age classes and gender, as sexually mature females typically moult later than males and young seals, therefore the period of vibrissa growth could also change in a similar manner.

The amount of ecological information that a vibrissa segment contains also depends on its location along the vibrissa. A segment closer to the base of the vibrissa has more information than a segment closer to the tip of the vibrissa and the difference can be tenfold (Beltran et al., 2015). This is due to the asymptotic growth pattern, where growth rates slow as the vibrissa approaches an asymptotic length. Therefore, understanding the importance of species-specific and vibrissa position-specific growth rates is crucial for analysis.

In summary, this study was the first to characterize the growth and shedding of harp seal vibrissae. The vibrissae had an asymptotic growth profile with an approximate one-year lifespan, and the mean period of growth was 104 days, occurring from late March until mid-July. The high variability in asymptotic lengths of the vibrissae limits the ability to use the same von Bertalanffy equations across seals, however knowing how the harp seal annual cycle aligns with the growth period will provide future researchers with valuable information for future ecological studies.

Table 2-1. The mean number of days for captive harp seal (*Pagophilus groenlandicus*) vibrissae to reach asymptotic lengths, calculated by breakpoint analysis in R software. The mean number of days, standard deviation, range, and sample size are listed by seal, vibrissa position, and vibrissa row.

Seal, vibrissa position, and vibrissa row	Days post shedding to reach asymptotic length (mean ± standard deviation)	Range (days)	N
Babette	103 ± 14.5	84 – 127	12
Tyler	109 ± 11.3	84 – 122	12
Deane	101 ± 8.8	78 – 127	12
A2	101 ± 14.3	84 – 121	6
A3	91 ± 3.8	84 – 93	6
B1	107 ± 15.9	78 – 122	6
B2	106 ± 13.2	84 – 122	6
C1	117 ± 13.9	99 – 127	6
C2	106 ± 13.3	93 – 122	6
Row A	96 ± 11.3	84 – 121	12
Row B	107 ± 14.0	78 – 122	12
Row C	111 ± 14.1	93 – 127	12
Overall	105 ± 14.4	78 – 127	36

Table 2-2. Maximal vibrissa growth rates (cm/day; mean ± 1 standard error) and date of maximal vibrissa growth for captive harp seals (*Pagophilus groenlandicus)* by vibrissa position.

Vibrissa	Maximal growth rate ± standard error (cm/day)	N	Date of maximal growth (in 2017)
Babette			
RA2	0.31 ± 0.02	42	11 April
RA3	0.27 ± 0.01	43	11 April
RB1	0.4 ± 0.03	43	13 July
RB2	0.36 ± 0.03	44	13 July
RC1	0.40 ± 0.03	41	04 August
RC2	0.37 ± 0.02	42	25 August
LA2	0.26 ± 0.02	41	11 April
LA3	0.25 ± 0.02	41	11 April
LB1	0.23 ± 0.01	41	27 April
LB2	0.24 ± 0.02	40	19 July
LC1	0.35 ± 0.03	41	13 July
LC2	0.26 ± 0.02	42	13 July
Tyler			
RA2	0.47 ± 0.02	46	05 April
RA3	0.24 ± 0.04	45	27 April
RB1	0.21 ± 0.04	44	27 April
RB2	0.22 ± 0.03	46	27 April
RC1	0.24 ± 0.02	43	31 May
RC2	0.25 ± 0.01	44	27 April
LA2	0.14 ± 0.01	43	12 October
LA3	0.28 ±0.02	45	24 May
LB1	0.23 ± 0.02	45	14 June
LB2	0.27 ± 0.02	43	24 May
LC1	0.28 ± 0.02	43	15 September
LC2	0.31 ± 0.02	44	27 April
Deane			
RA2	0.23 ± 0.02	45	11 April
RA3	0.20 ± 0.01	45	11 April
RB1	0.29 ± 0.02	42	6 June
RB2	0.24 ± 0.02	45	11 April
RC1	0.36 ± 0.03	43	27 April
RC2	0.33 ± 0.02	41	27 July

Vibrissa	Maximal growth rate ± standard error (cm/day)	N	Date of maximal growth (in 2017)
Deane			
LA2	0.29 ± 0.03	47	19 April
LA3	0.28 ± 0.02	46	16 October
LB1	0.38 ± 0.04	47	12 October
LB2	0.24 ± 0.02	46	19 July
LC1	0.42 ± 0.02	39	11 August
LC2	0.24 ± 0.03	45	19 April

Table 2-3. The coefficient of variation (%) describing the measurement precision and repeatability of the triplicate vibrissa length measurements for each vibrissa on each sampling event. The mean coefficient of variation (%) and sample size is listed for each seal, vibrissa position and row.

Seal, vibrissa position, and vibrissa row	Coefficient of variation (%)	N
Babette	7.6	502
Tyler	4.9	546
Deane	5.8	508
A2	4.5	264
A3	5.6	267
B1	5.6	264
B2	4.8	266
C1	9.3	245
C2	6.8	250
Row A	5.1	531
Row B	5.2	530
Row C	8.0	495
Overall	6.1	1556

Table 2-4. The dates that captive harp seal (*Pagophilus groenlandicus*) vibrissae were shed in 2017 and 2018, and the vibrissa lifespan for each vibrissa position. Lifespan estimates are limited to the sampling interval listed in the "Shedding date 1" and Shedding date 2".

Vibrissa	Shedding date 1 (2017)	Shedding date 2 (2018)	Lifespan (days)
Babette			
RA2	Prior to 05 April	05 March - 27 March	>349
RA3	Prior to 05 April	05 March - 27 March	>349
RB1	Prior to 05 April	05 March - 27 March	>349
RB2	06 April - 11 April	28 March - 04 April	364
RC1	Prior to 05 April	05 March - 27 March	>349
RC2	06 April - 11 April	28 March - 04 April	364
LA2	Prior to 05 April	05 March - 27 March	>349
LA3	Prior to 05 April	05 March - 27 March	>349
LB1	Prior to 05 April	05 March - 27 March	>349
LB2	Prior to 05 April	05 March - 27 March	>349
LC1	Prior to 05 April	05 March - 27 March	>349
LC2	06 April - 11 April	28 March - 04 April	364
Tyler			
RA2	Prior to 05 April	05 March - 27 March	>349
RA3	06 April - 11 April	05 March - 27 March	357
RB1	06 April - 11 April	05 March - 27 March	357
RB2	06 April - 11 April	Not shed as of 04 April	NA
RC1	12 April - 19 April	Not shed as of 04 April	NA
RC2	12 April - 19 April	Not shed as of 04 April	NA
LA2	12 April - 19 April	Not shed as of 04 April	NA
LA3	Prior to 05 April	05 March - 27 March	>357
LB1	Prior to 05 April	05 March - 27 March	>357
LB2	12 April - 19 April	Not shed as of 04 April	NA
LC1	12 April - 19 April	Not shed as of 04 April	NA
LC2	12 April - 19 April	Not shed as of 04 April	NA
Deane			
RA2	Prior to 05 April	05 March - 27 March	>357
RA3	Prior to 05 April	ND	NA
RB1	Prior to 05 April	ND	NA
RB2	Prior to 05 April	ND	NA
RC1	12 April - 19 April	ND	NA
RC2	12 April - 19 April	ND	NA
LA2	Prior to 05 April	28 March - 04 April	>364
LA3	Prior to 05 April	28 March - 04 April	>364
LB1	Prior to 05 April	28 March - 04 April	>364

Vibrissa	Shedding date 1 (2017)	Shedding date 2 (2018)	Lifespan (days)
Deane			
LB2	Prior to 05 April	28 March - 04 April	>364
LC1	Prior to 05 April	05 March - 27 March	>349
LC2	06 April - 11 April	28 March - 04 April	364

ND represents vibrissae that were not measured on the last day of the study; therefore, no data is available.

NA represents vibrissae that shed before the beginning of the study or did not shed by the end of the study, and therefore, lifespan could not be calculated.

Table 2-5. Number of vibrissae shed during 2017 and 2018 for captive harp seals (*Pagophilus groenlandicus*), *Babette, Tyler,* and *Deane.* The number of vibrissae shed per seal, and total vibrissae shed on each date are listed.

Seal	Shedding date	Number of vibrissae shed	Total vibrissae shed on each date
Babette	06 April - 11 April 2017	3	
Tyler		3	7
Deane		1	
Babette	12 April - 19 April 2017	0	
Tyler		6	8
Deane		2	
Babette	05 March - 27 March 2018	9	
Tyler		5	16
Deane		2	
Babette	28 March - 4 April 2018	3	
Tyler		0	8
Deane		5	

Table 2-6. Estimates of von Bertalanffy coefficients describing vibrissa growth for captive harp seals (*Pagophilus groenlandicus*). Estimates for growth coefficients K, asymptotic length L_∞, and time of initial growth T_o are listed by vibrissa position.

Vibrissa	K	L_∞	T_o
Babette			
RA2	0.028	9.79	2.67
RA3	0.031	8.23	2.73
RB1	0.021	10.52	3.09
RB2	0.030	9.11	1.09
RC1	0.014	8.91	2.90
RC2	0.022	6.44	-0.13
LA2	0.031	9.25	3.12
LA3	0.034	7.73	2.78
LB1	0.023	11.18	3.84
LB2	0.029	9.33	3.25
LC1	0.020	9.46	3.33
LC2	0.025	7.63	3.99
Tyler			
RA2	0.033	9.96	-0.77
RA3	0.030	8.67	-3.76
RB1	0.021	12.62	-7.60
RB2	0.022	10.95	3.03
RC1	0.024	9.89	1.25
RC2	0.025	8.85	1.39
LA2	0.021	5.61	6.60
LA3	0.025	7.80	0.74
LB1	0.021	12.20	-0.87
LB2	0.022	10.43	1.00
LC1	0.020	10.96	2.10
LC2	0.026	7.93	3.68
Deane			
RA2	0.023	11.22	1.06
RA3	0.026	9.13	1.95
RB1	0.020	12.16	4.14
RB2	0.022	10.99	2.75
RC1	0.022	9.98	-3.74
RC2	0.033	7.54	-4.66
LA2	0.025	11.04	0.80
LA3	0.025	8.91	1.09
LB1	0.032	10.13	2.93
LB2	0.024	10.72	2.77

Vibrissa	K	L_∞	T_0
Deane			
LC1	0.017	8.56	5.53
LC2	0.032	7.33	-0.10

K represents the growth constant,

L_∞ represents the asymptotic length,

T_0 represents the time of initial growth. Negative values are due to vibrissae that had a measurable growth on Day 1 of the experiment. Therefore, the initial time of growth would occur before Day 1.

Table 2-7. Asymptotic lengths (cm; mean ± 1 standard error) of vibrissae in the two posterior

positions in rows A, B, and C for captive harp seals (*Pagophilus groenlandicus*), *Babette, Tyler,*

and *Deane*.

Vibrissa	Relative position	Mean ± standard error (cm)	N	Range (cm)
A2	Posterior	9.5 ± 0.86	6	5.6 [T] – 11.2 [D]
A3	Medial	8.4 ± 0.23	6	7.7 [B] – 9.1 [D]
B1	Posterior	11.5 ± 0.46	6	10.1 [D] – 12.6 [T]
B2	Medial	10.3 ± 0.41	6	9.1 [B] – 11.0 [D]
C1	Posterior	9.6 ± 0.37	6	8.6 [D] – 11.0 [T]
C2	Medial	7.6 ± 0.35	6	6.4 [B] – 8.9 [T]

The superscript text indicates the seal associated with the asymptotic length: B, T, and D
represent *Babette, Tyler* and *Deane*, respectively. Vibrissa lengths are derived from the estimated
asymptotic length of von Bertalanffy equations fitted to vibrissa length measurements.

Table 2-8. Likelihood ratio tests were used to compare the parameter estimates of the von Bertalanffy growth model for the two posterior macrovibrissae in rows A, B, and C of captive harp seals (*Pagophilus groenlandicus*), *Babette*, *Tyler*, and *Deane*. Likelihood ratio tests compared the parameter estimates on the left and right side within each seal and the P-values are listed.

Vibrissa Position	L_∞	K	T_0	All parameters
Babette				
A2	0.001	0.380*	0.806*	0.010
A3	0.001	0.556*	1.000*	0.004
B1	0.003	0.315*	0.718*	0.000
B2[1]	0.198*	0.752*	0.183*	0.202*
C1	0.180*	0.035	0.862*	0.000
C2	0.000	0.450*	0.206*	0.000
Tyler				
A2	0.000	0.000	0.000	0.000
A3	0.000	0.112*	0.806*	0.000
B1	0.024	0.584*	0.549*	0.001
B2	0.000	0.888*	0.001	0.000
C1	0.000	0.332*	0.708*	0.000
C2	0.000	0.578*	0.365*	0.000
Deane				
A2[1]	0.823*	0.671*	0.718*	0.849*
A3[1]	0.127*	0.655*	0.888*	0.177*
B1	0.000	0.000	0.841*	0.000
B2[1]	0.068*	0.322*	0.888*	0.316*
C1	0.000	0.507*	0.390*	0.000
C2[1]	0.142*	0.888*	0.396*	0.337*

[1] Denotes vibrissae where the null hypothesis was not rejected at the $p = 0.05$ significance level for all von Bertalanffy parameter estimates, implying no difference between left and right vibrissae.

* Indicates the null hypothesis was not rejected at the $p = 0.05$ significance level.

Table 2-9. Likelihood ratio tests were used to compare the parameter estimates of the von Bertalanffy growth model for the two posterior macrovibrissae in rows A, B, and C across three captive harp seals (*Pagophilus groenlandicus*). P-values are listed from testing parameter estimates against a null hypothesis to determine if von Bertalanffy equations can be shared across seals.

Vibrissa Position	L_∞	K	T_0	All parameters
A2	0.000	0.000	0.000	0.000
A3	0.000	0.273*	0.934*	0.000
B1	0.000	0.000	0.098*	0.000
B2	0.000	0.000	0.000	0.000
C1	0.000	0.045	0.003	0.000
C2	0.000	0.870*	0.001	0.000

*An asterisk indicates that the null hypothesis was not rejected at the $p=0.05$ significance level.

Table 2-10. Vibrissa growth rates and shedding patterns are species-specific among phocids and otariids. Vibrissa growth and shedding are separated by species and study (after McHuron et al. (2016)).

Species	Growth rate (cm/day)	Asymptotic length (cm)	Growth pattern	Method of measurement	Shedding	Citation
Otariids						
Steller sea lion	0.015 ± 0.005 (A)	NA	linear	isotope oscillations	NA	Rea et al. (2015)
California sea lion	0.007 ± 0.004 (A)	NA	linear	photogrammetry	NA	McHuron et al. (2016)
Antarctic fur seal	0.005 – 0.008	NA	linear	isotope oscillations	NA	Kernaléguen et al. (2012)
Phocids						
Harbour seal	0.0075 (A)	6.0 – 10.0	asymptotic	isotope tracers	seasonal	Zhao and Schell (2004)
Harbour seal	0.008 – 0.037 (A)	6.0 – 9.0	irregular	isotope matching/tracers	NA	Hirons et al. (2001)
Harbour seal	0.046 –0.145	6.97 – 11.74	asymptotic	photogrammetry	April-August	Karpovich et al. (2022)
Bearded seal	0.030 – 0.120	3.0 – 22.2*	rapid-slow	photogrammetry	no temporal pattern	McHuron et al. (2020)

Species	Growth rate (cm/day)	Asymptotic length (cm)	Growth pattern	Method of measurement	Shedding	Citation
Northern elephant seal	0.013 ± 0.007 (A)	2.0 – 16.4	asymptotic	photogrammetry	no temporal pattern	Beltran et al. (2015)
Northern elephant seal	0.007 – 0.100	4.8 – 14.2	non-linear	photogrammetry	seasonal	McHuron et al. (2018)
Southern elephant seal	0.047 – 0.067	4.75 – 15.43	asymptotic	clip/regrow	seasonal	Lübcker et al. (2016)
Grey seal	0.024	5.8 ± 0.3	asymptotic	photogrammetry	no temporal pattern	Greaves et al. (2004)
Spotted seal	0.036 ± 0.015 (SA)	6.2 ± 3.1	asymptotic	photogrammetry	seasonal	McHuron et al. (2016)
Ringed seal	0.04 – 0.15	1.0 – 8.9	asymptotic	photogrammetry	seasonal	McHuron et al. (2020)
Hawaiian monk seal	0.030 – 0.100	1.9 - 22.1*	rapid-slow	photogrammetry	no temporal pattern	McHuron et al. (2020)
Harp seal	0.14 – 0.47	5.6 – 12.6	asymptotic	photogrammetry	seasonal	present study

Values with an asterisk * denote maximal vibrissa lengths since growth was not asymptotic.

Growth rates are presented as mean ± standard deviation or a minimum-maximum range.

A; adult animals,

SA; subadults.

NA; not applicable

Figure 2-1. The body mass (kg) of captive harp seals (*Pagophilus groenlandicus*) *Babette*, *Tyler*, and *Deane* measured over one year.

Figure 2-2. Captive seals were trained to rest their chin on a wooden spherical target for photography. The centimeter scale bar (see Figure 2-3) is below the target and perpendicular to the camera.
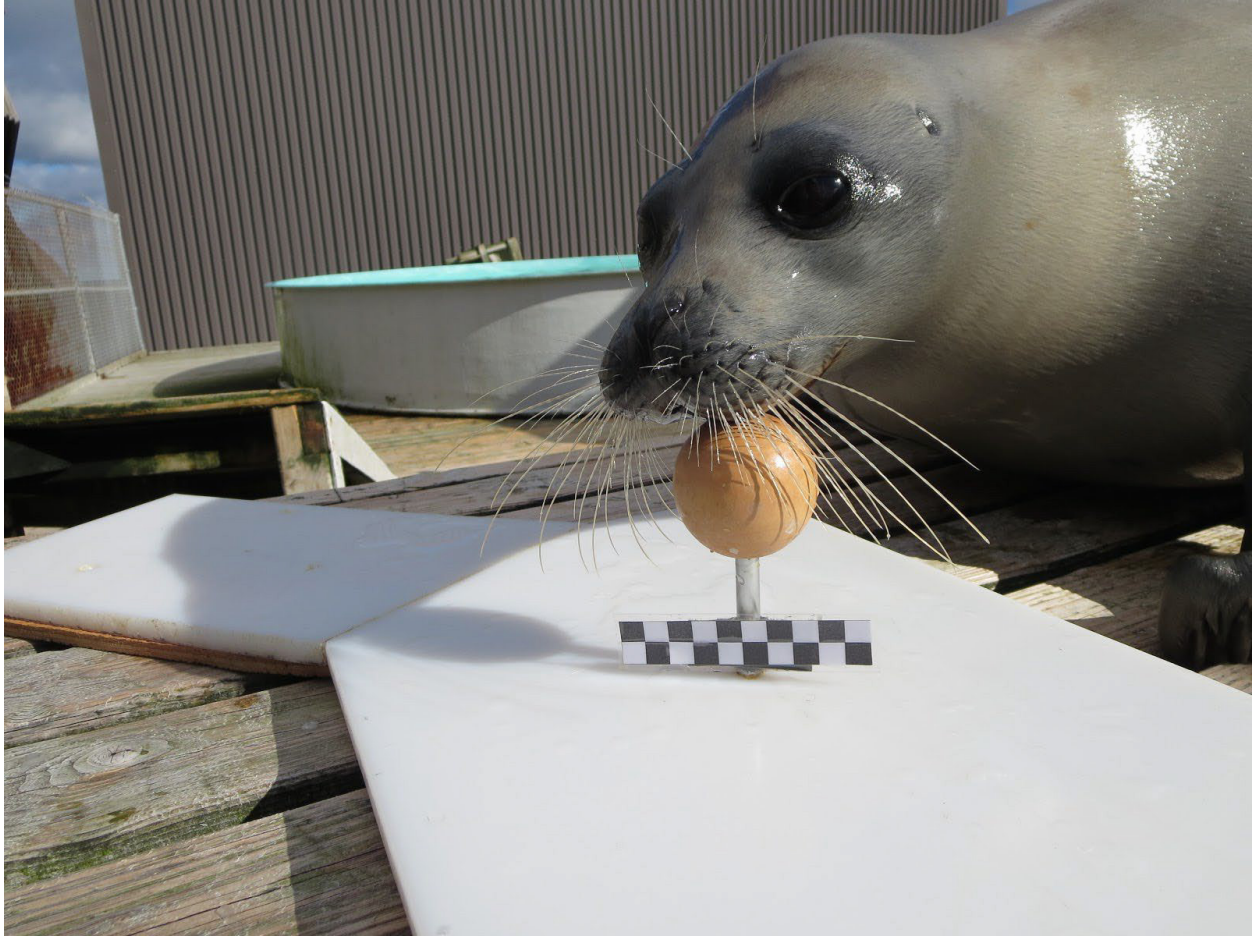
Figure 2-3. *Deane*, a captive harp seal (*Pagophilus groenlandicus*), rests her chin on the

wooden target for a vibrissa photogrammetry session. The scale bar, where each black square

represents one centimeter, is perpendicular to the camera.
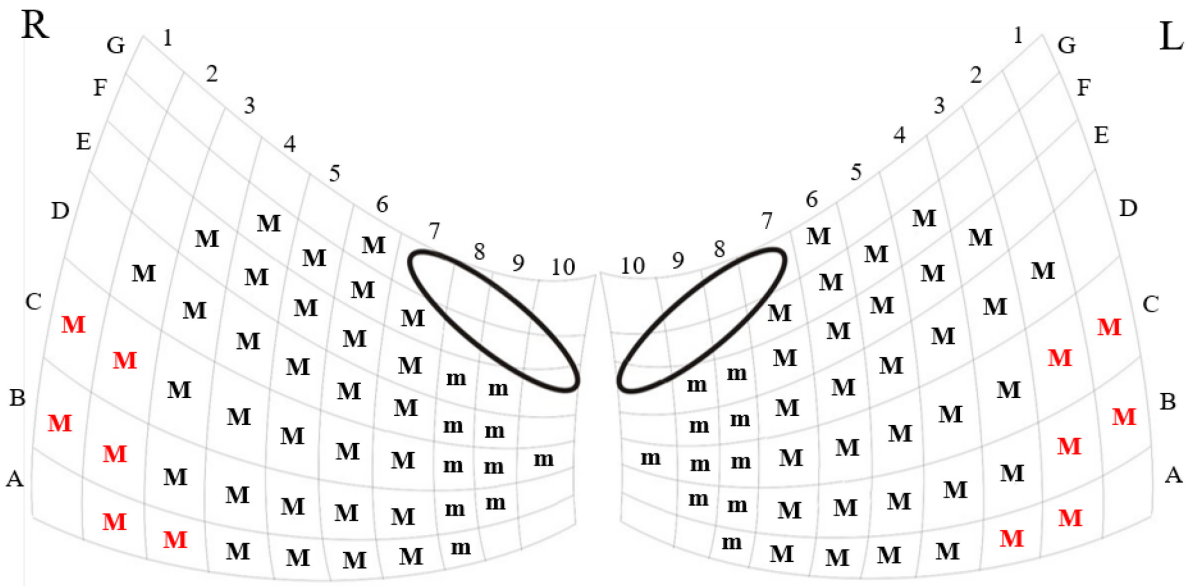
Figure 2-4. Standardized diagram of microvibrissae (m) and macrovibrissae (M) showing the distribution of vibrissae into rows and columns. The ellipses represent the seal's nostrils and red letters represent macrovibrissae measured in this study.
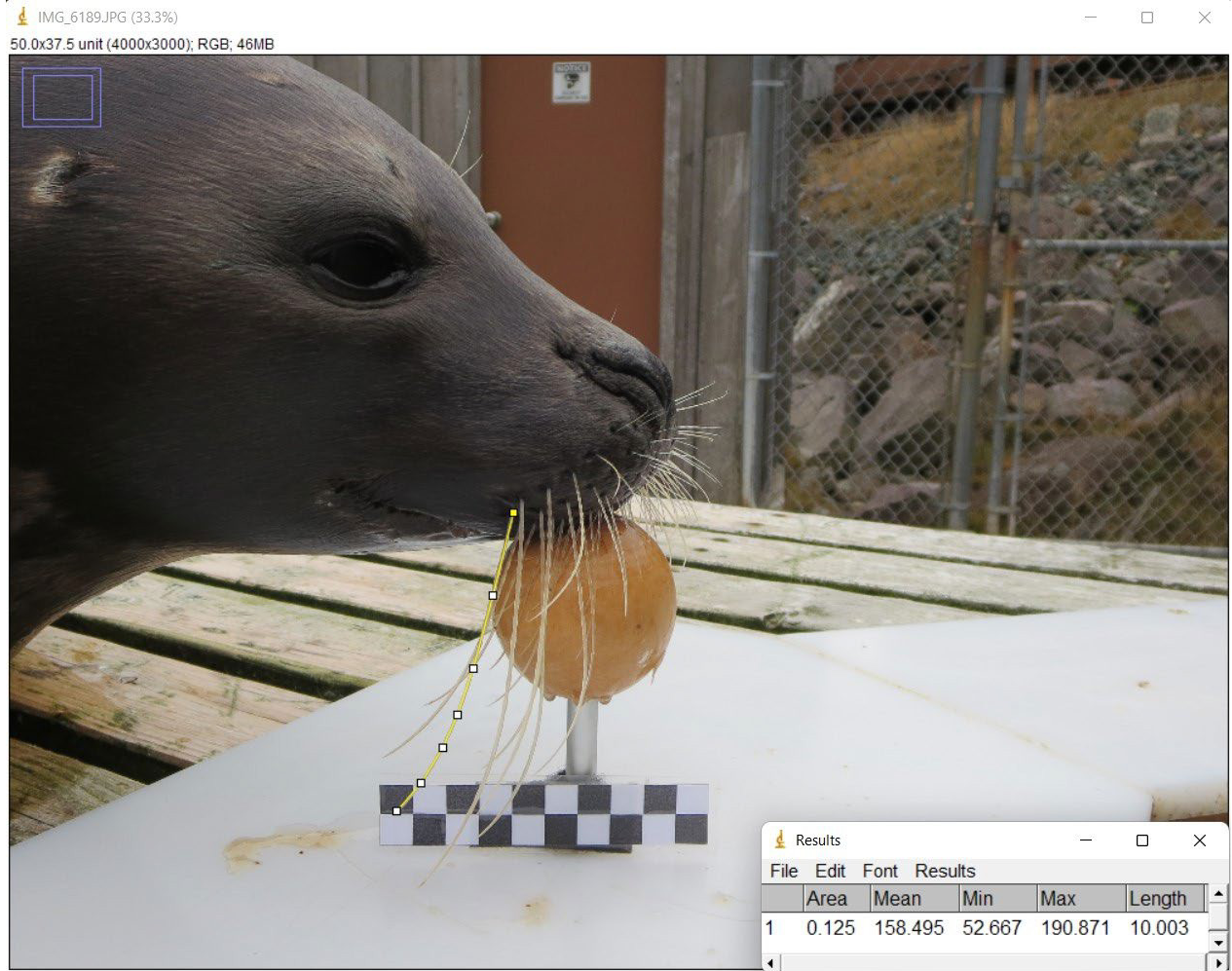
Figure 2-5. Photographs of vibrissae are measured in Image Processing and Analysis in Java (ImageJ) software using the segmented line tool to follow the natural curve of the vibrissa (Schneider et al., 2012).
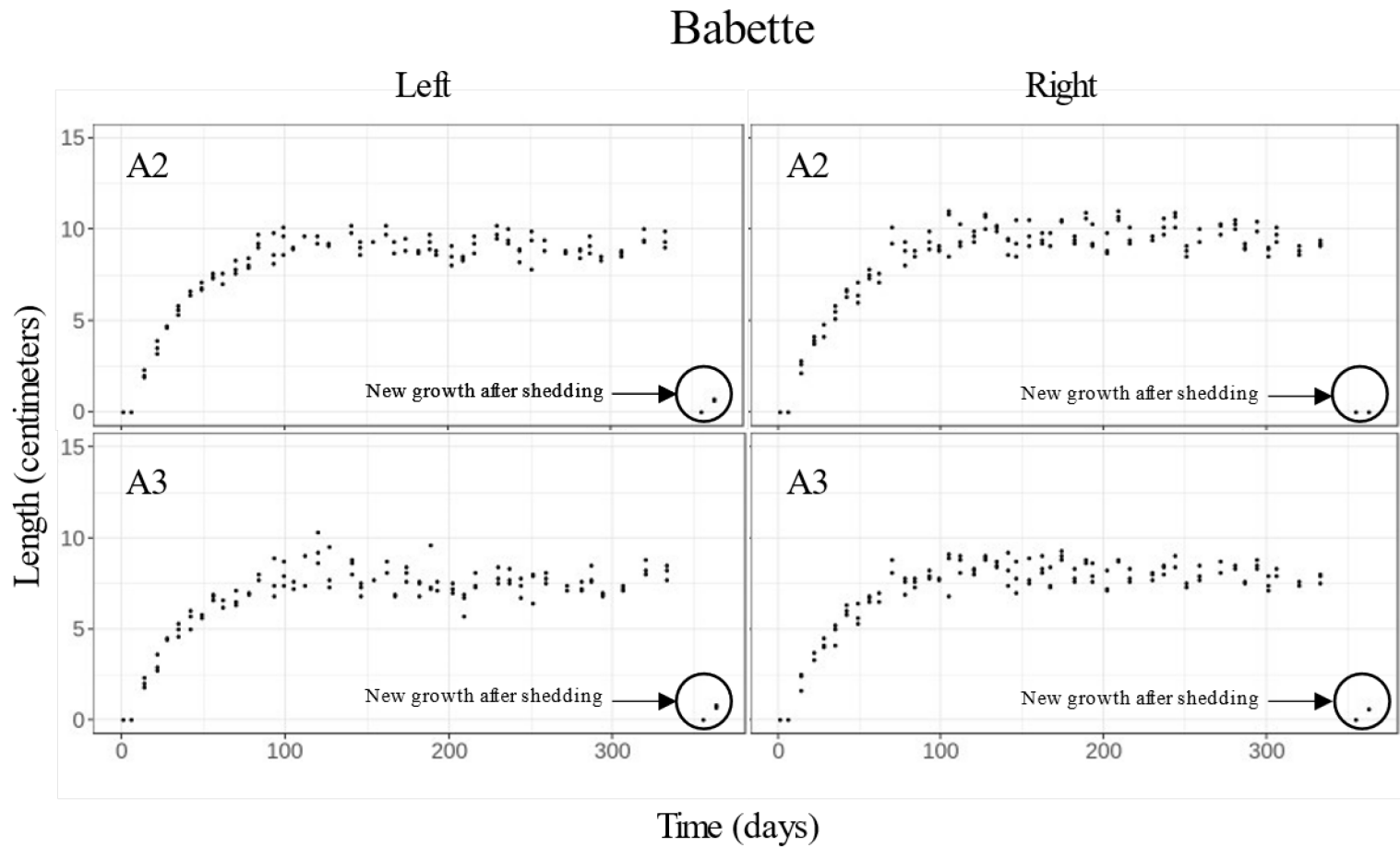
Figure 2-6A. Triplicate vibrissa length measurements for captive harp seal (*Pagophilus groenlandicus*), *Babette*. The two posterior macrovibrissae in row A were measured on the left and right side of the face. Circles mark new growth of vibrissa post-shedding.
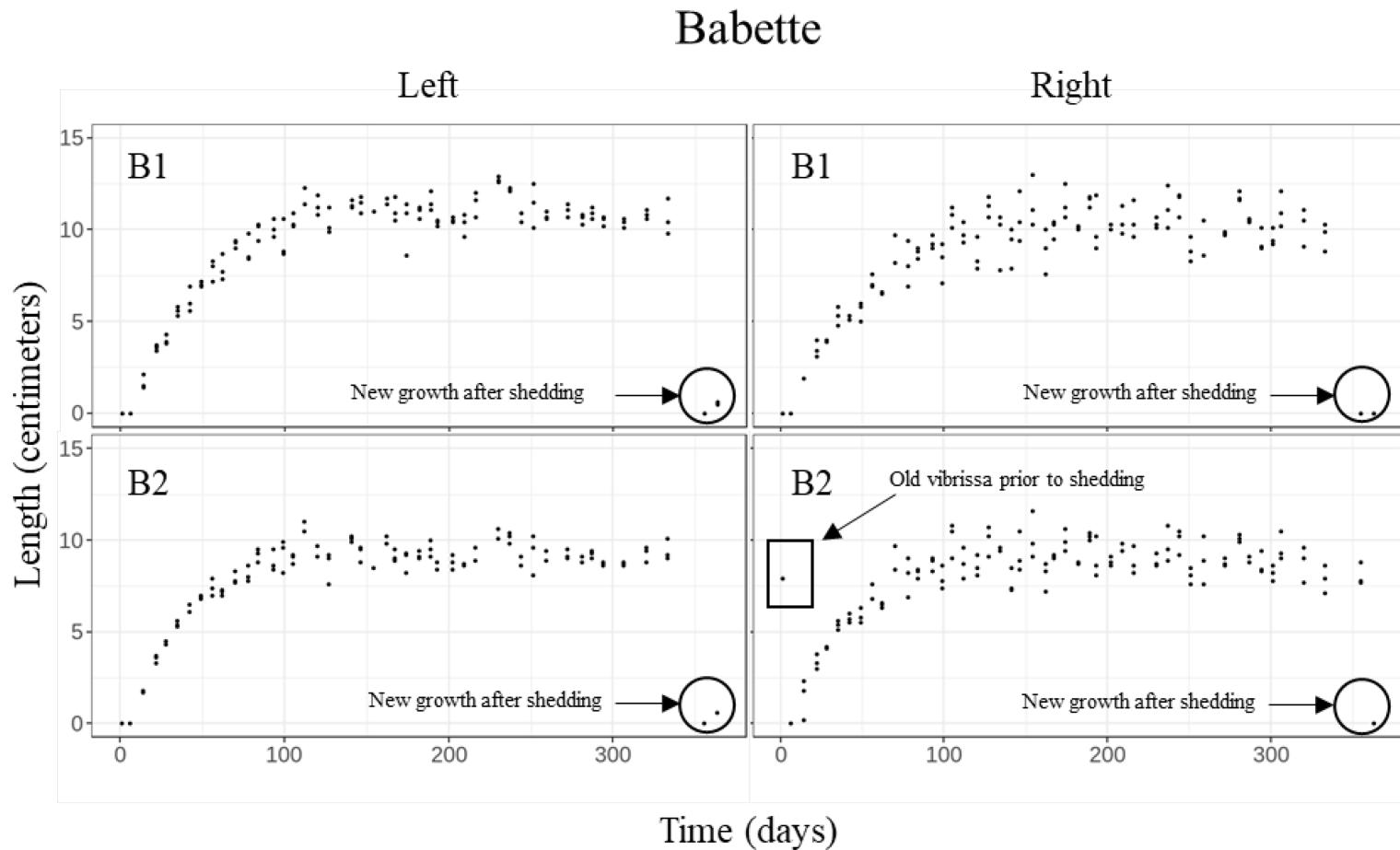
Figure 2-6B. Triplicate vibrissa length measurements for captive harp seal (*Pagophilus groenlandicus*), *Babette*. The two posterior macrovibrissae in row B were measured on the left and right side of the face. Circles mark new growth of vibrissa post-shedding; lengths of old vibrissae before shedding are marked by boxes.
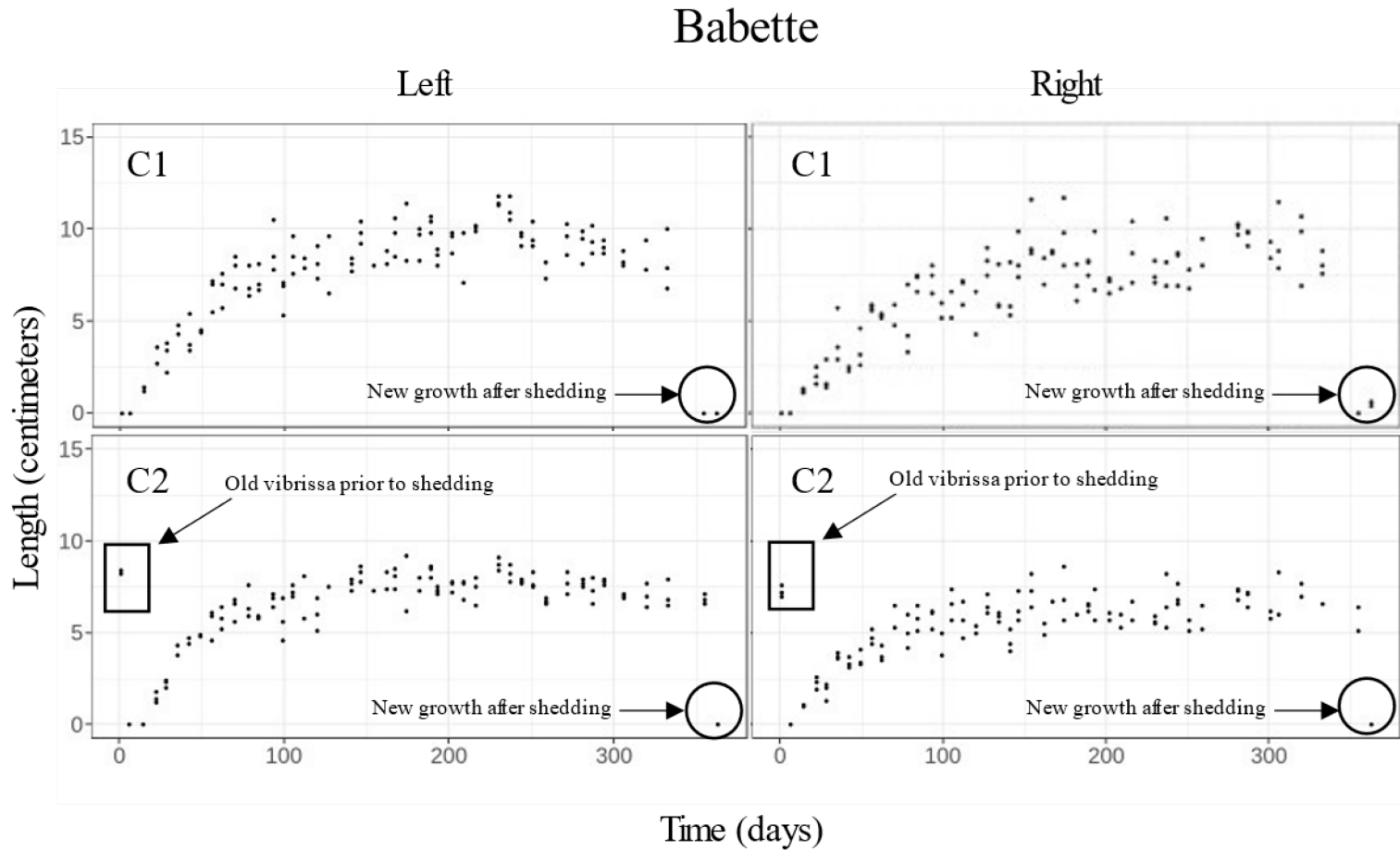
Figure 2-6C Triplicate vibrissa length measurements for captive harp seal (*Pagophilus groenlandicus*), *Babette*. The two posterior macrovibrissae in row C were measured on the left and right side of the face. Circles mark new growth of vibrissa post-shedding; lengths of old vibrissae before shedding are marked by boxes.
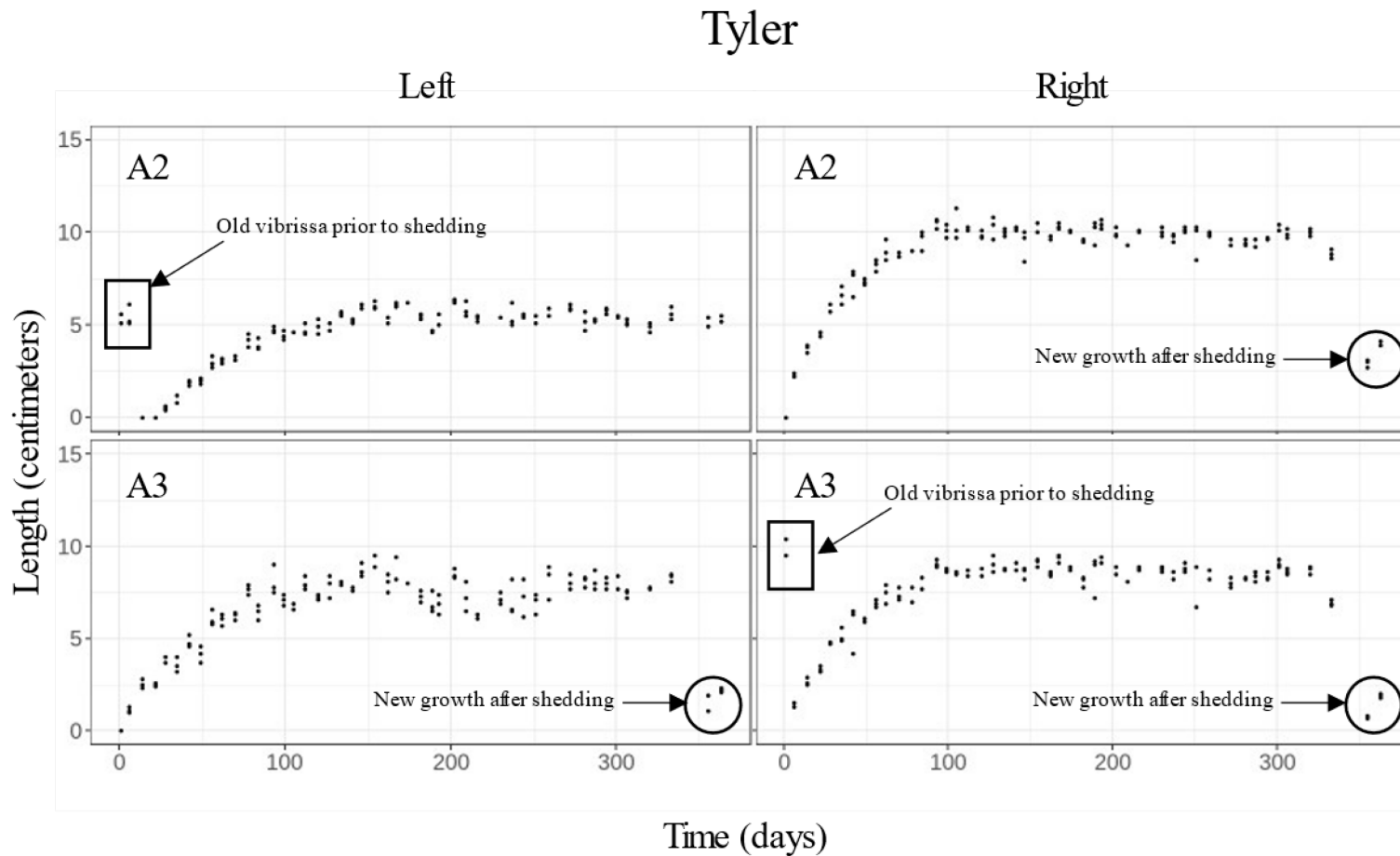
Figure 2-6D. Triplicate vibrissa length measurements for captive harp seal (*Pagophilus groenlandicus*), *Tyler*. The two posterior macrovibrissae in row A were measured on the left and right side of the face. Circles mark new growth of vibrissa post-shedding; lengths of old vibrissae before shedding are marked by boxes.

Figure 2-6E. Triplicate vibrissa length measurements for captive harp seal (*Pagophilus groenlandicus*), *Tyler*. The two posterior macrovibrissae in row B were measured on the left and right side of the face. Circles mark new growth of vibrissa post-shedding; lengths of old vibrissae before shedding are marked by boxes.
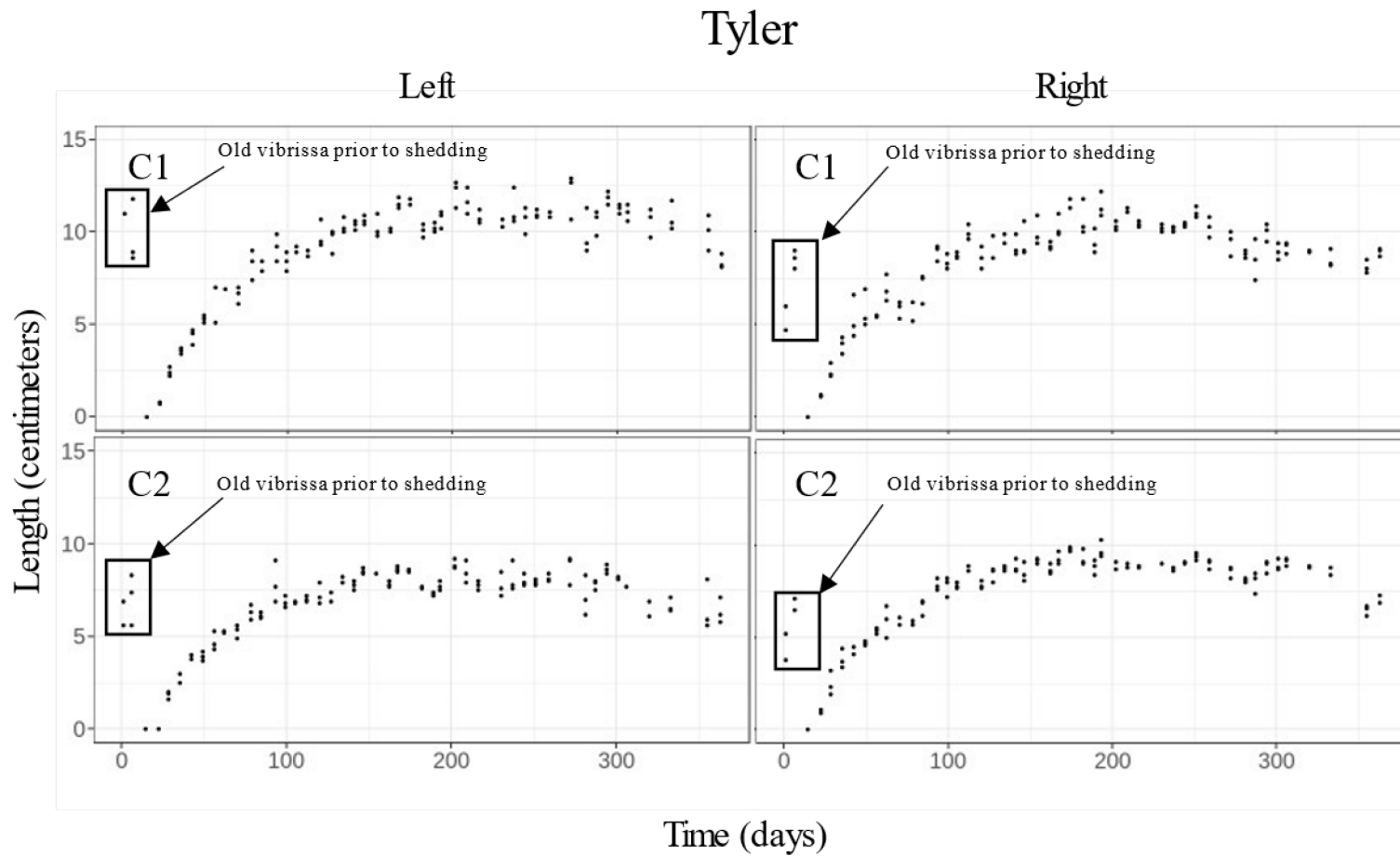
Figure 2-6F. Triplicate vibrissa length measurements for captive harp seal (*Pagophilus groenlandicus*), *Tyler*. The two posterior macrovibrissae in row C were measured on the left and right side of the face. Circles mark new growth of vibrissa post-shedding; lengths of old vibrissae before shedding are marked by boxes.
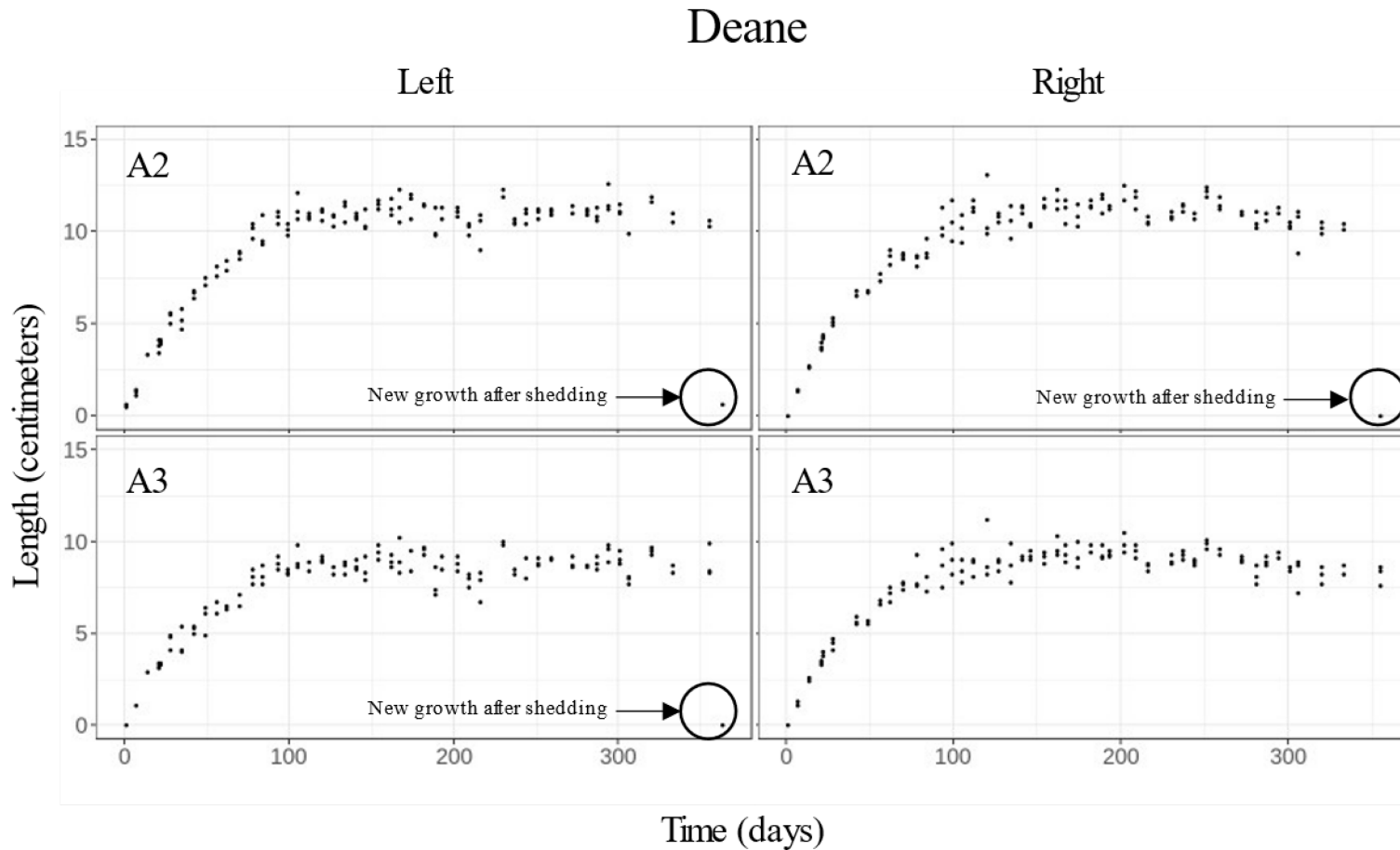
Figure 2-6G. Triplicate vibrissa length measurements for captive harp seal (*Pagophilus groenlandicus*), *Deane*. The two posterior macrovibrissae in row A were measured on the left and right side of the face. Circles mark new growth of vibrissa post-shedding.
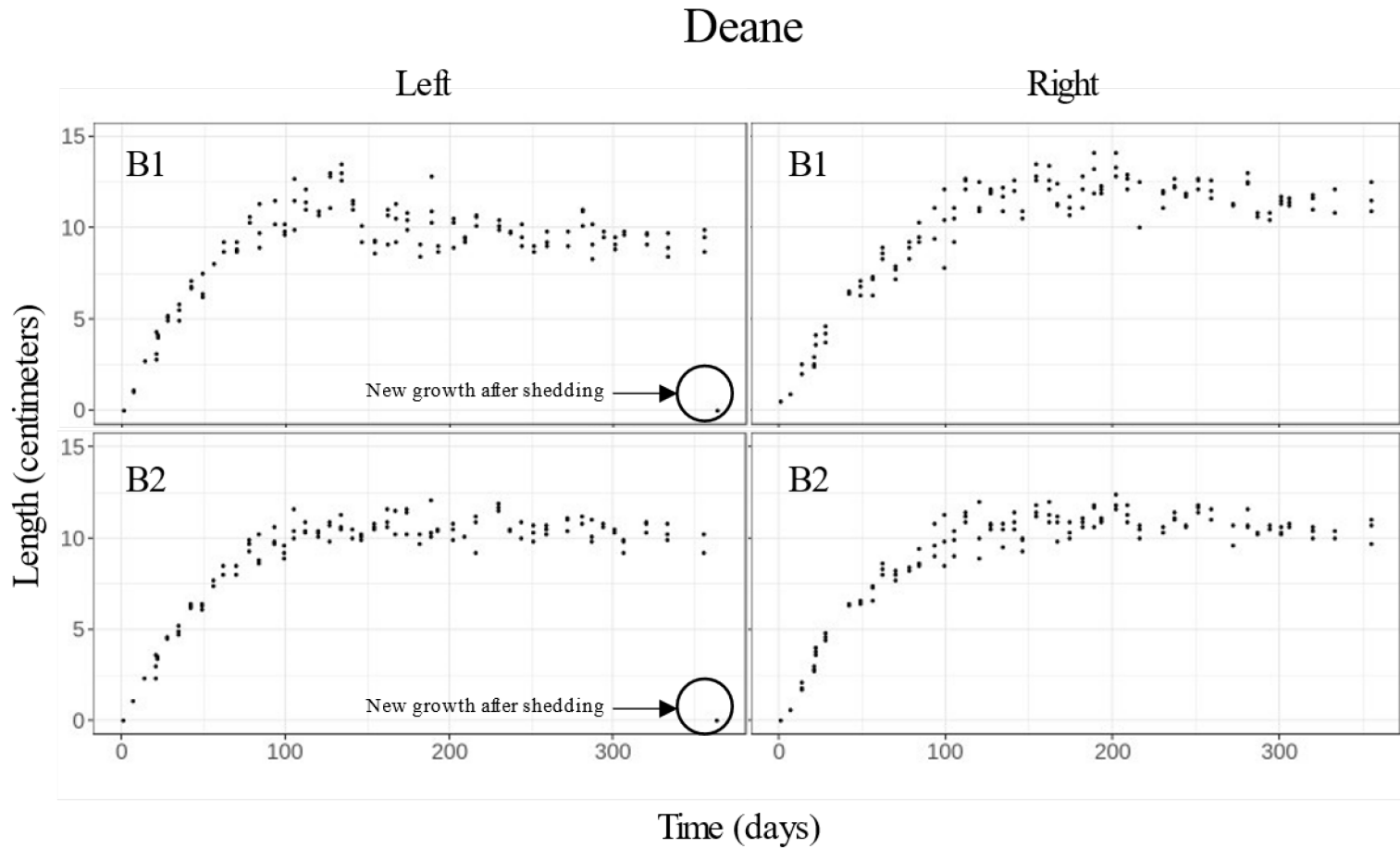
Figure 2-6H. Triplicate vibrissa length measurements for captive harp seal (*Pagophilus groenlandicus*), *Deane*. The two posterior macrovibrissae in row B were measured on the left and right side of the face. Circles mark new growth of vibrissa post-shedding.
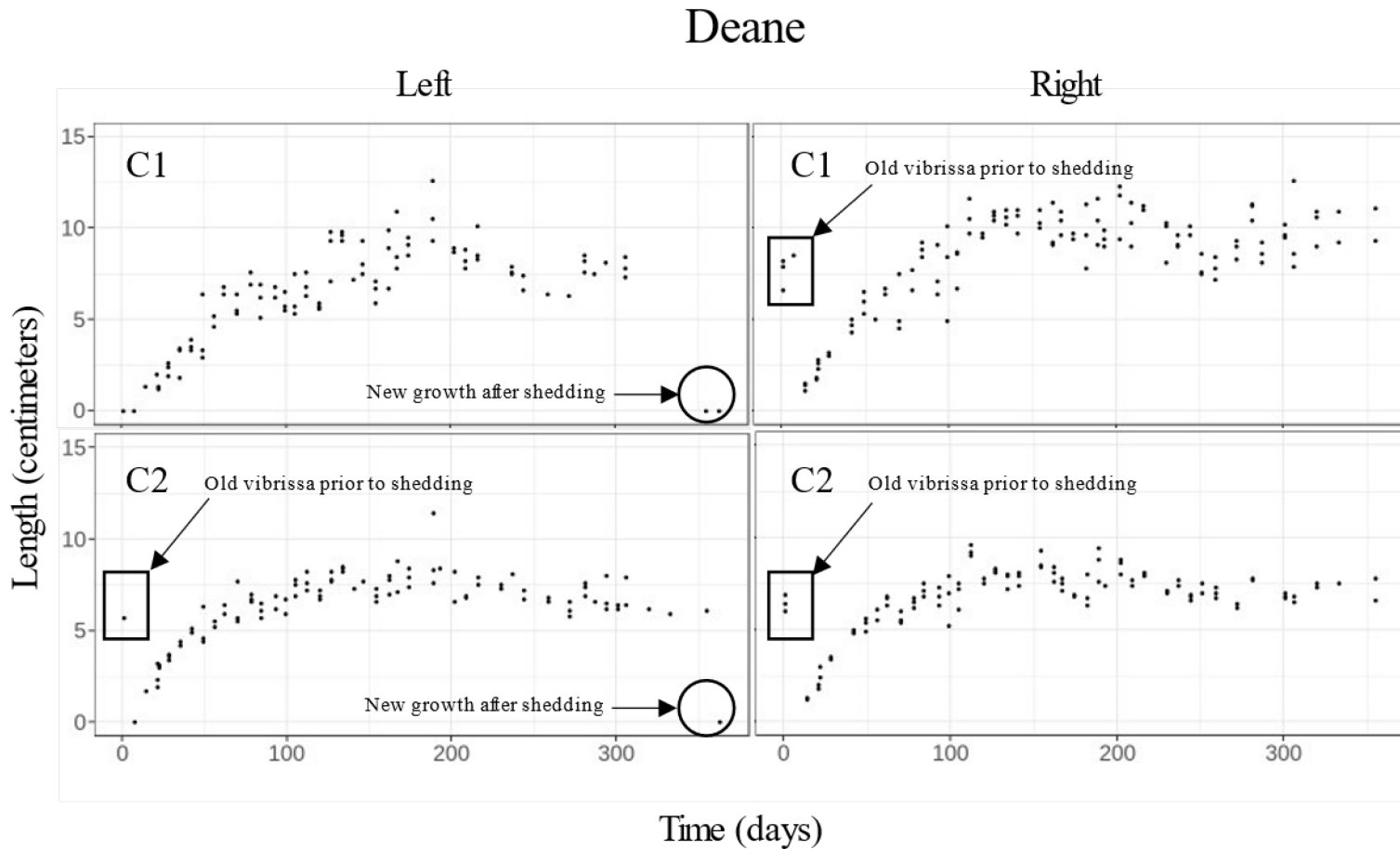
Figure 2-6I. Triplicate vibrissa length measurements for captive harp seal (*Pagophilus groenlandicus*), *Deane*. The two posterior macrovibrissae in row C were measured on the left and right side of the face. Circles mark new growth of vibrissa post-shedding; lengths of old vibrissae before shedding are marked by boxes.

Babette

| Left | Right |

A2 — $L_t = 9.25 \cdot (1 - e^{-0.031(T - 3.12)})$

A2 — $L_t = 9.79 \cdot (1 - e^{-0.028(T - 2.67)})$

A3 — $L_t = 7.73 \cdot (1 - e^{-0.034(T - 2.78)})$

A3 — $L_t = 8.23 \cdot (1 - e^{-0.031(T - 2.73)})$

Length (centimeters) — Time (days)
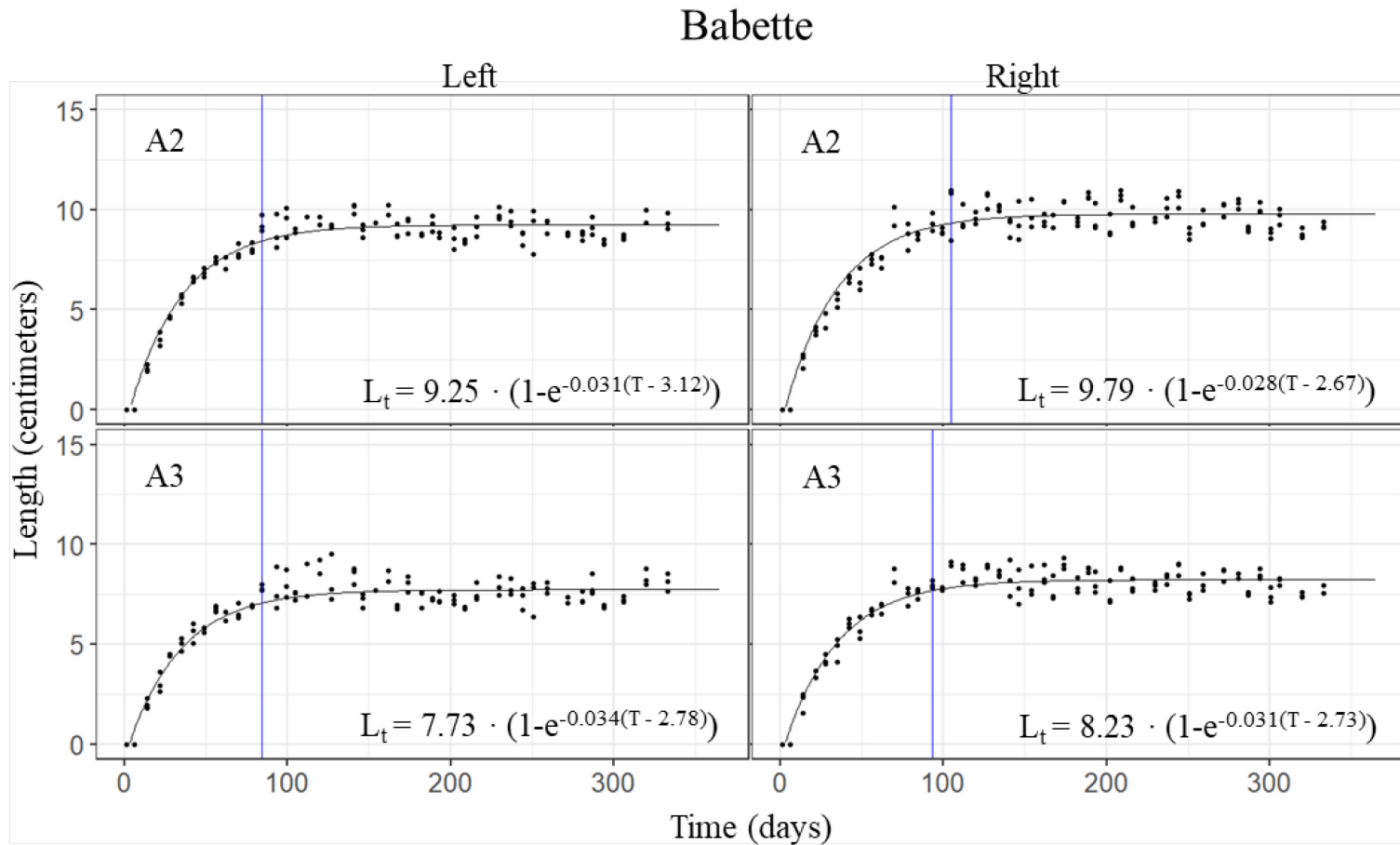
Figure 2-7A. von Bertalanffy equations fitted to the triplicate vibrissa length data for the two posterior macrovibrissae in row A for captive harp seal (*Pagophilus groenlandicus*), *Babette.* von Bertalanffy equations are listed in the bottom right corner for each vibrissa. The blue vertical line represents the breakpoint when the vibrissa reached an asymptotic length.

Babette

Left   Right

B1: $L_t = 11.18 \cdot (1-e^{-0.023(T-3.84)})$

B1: $L_t = 10.52 \cdot (1-e^{-0.021(T-3.09)})$

B2: $L_t = 9.33 \cdot (1-e^{-0.029(T-3.25)})$

B2: $L_t = 9.11 \cdot (1-e^{-0.030(T-1.09)})$

Length (centimeters) / Time (days)
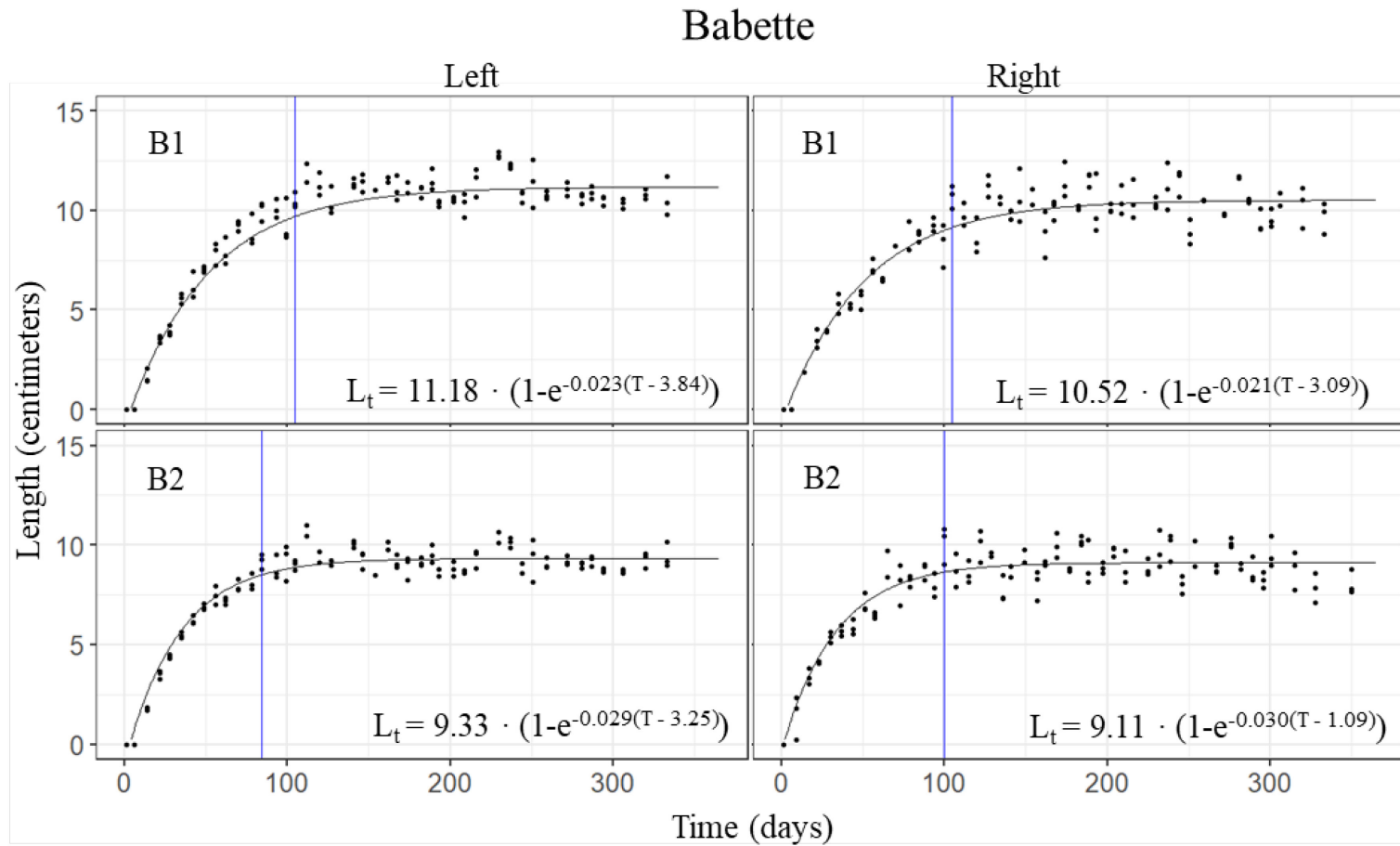
Figure 2-7B. von Bertalanffy equations fitted to the triplicate vibrissa length data for the two posterior macrovibrissae in row B for captive harp seal (*Pagophilus groenlandicus*), *Babette.* von Bertalanffy equations are listed in the bottom right corner for each vibrissa. The blue vertical line represents the breakpoint when the vibrissa reached an asymptotic length.
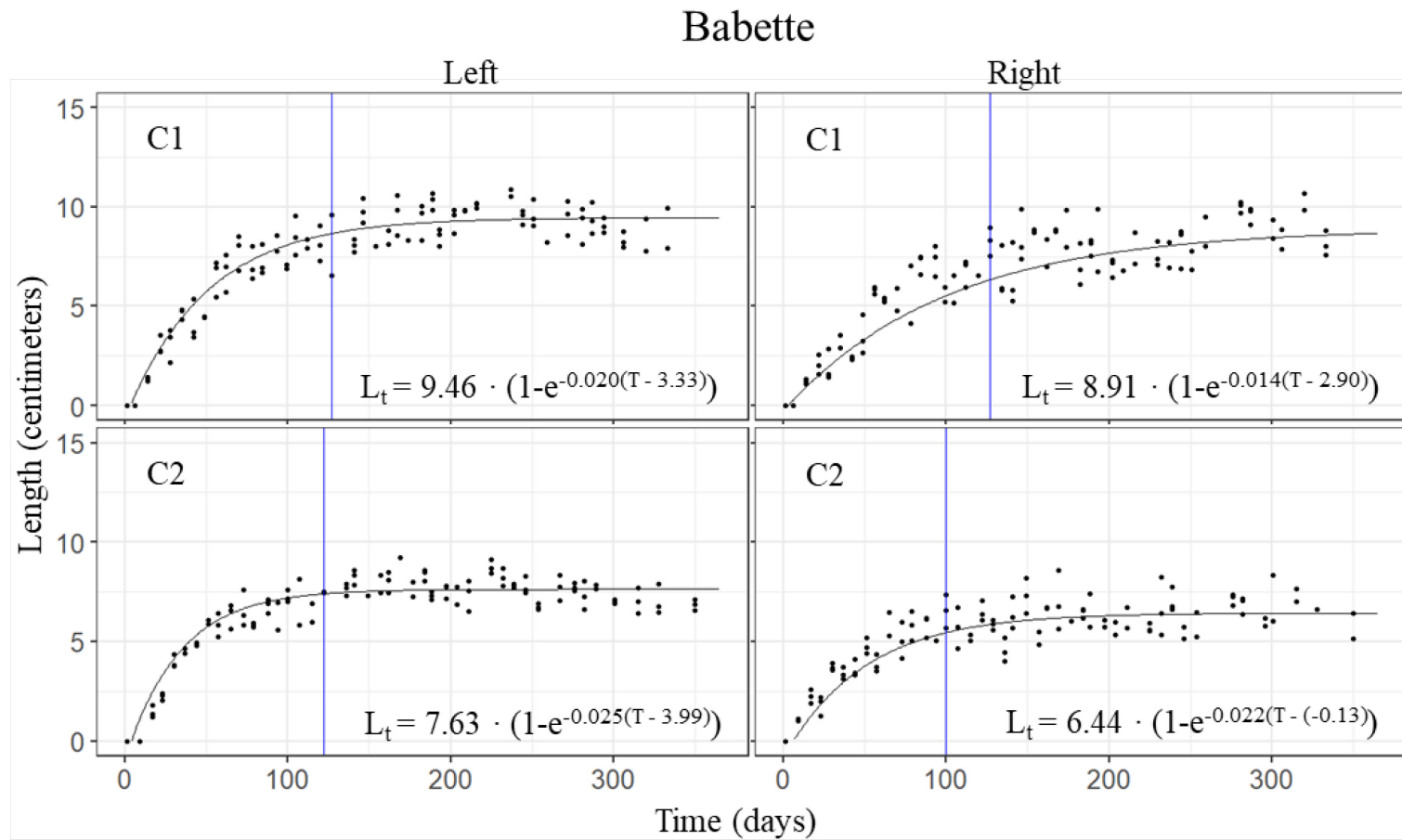
Figure 2-7C. von Bertalanffy equations fitted to the triplicate vibrissa length data for the two posterior macrovibrissae in row C for captive harp seal (*Pagophilus groenlandicus*), *Babette.* von Bertalanffy equations are listed in the bottom right corner for each vibrissa. The blue vertical line represents the breakpoint when the vibrissa reached an asymptotic length.
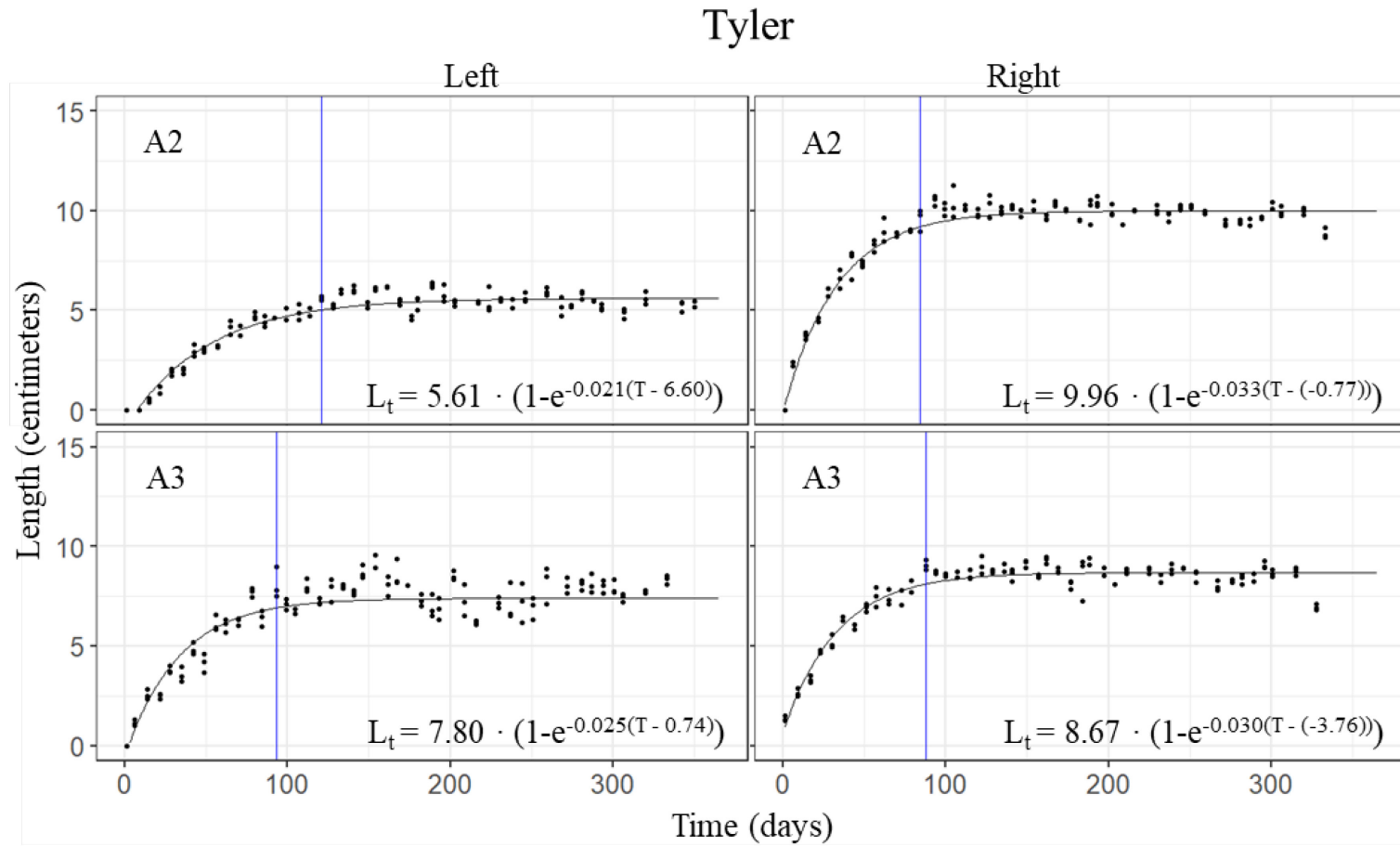
Figure 2-7D. von Bertalanffy equations fitted to the triplicate vibrissa length data for the two posterior macrovibrissae in row A for captive harp seal (*Pagophilus groenlandicus*), *Tyler*. von Bertalanffy equations are listed in the bottom right corner for each vibrissa. The blue vertical line represents the breakpoint when the vibrissa reached an asymptotic length.
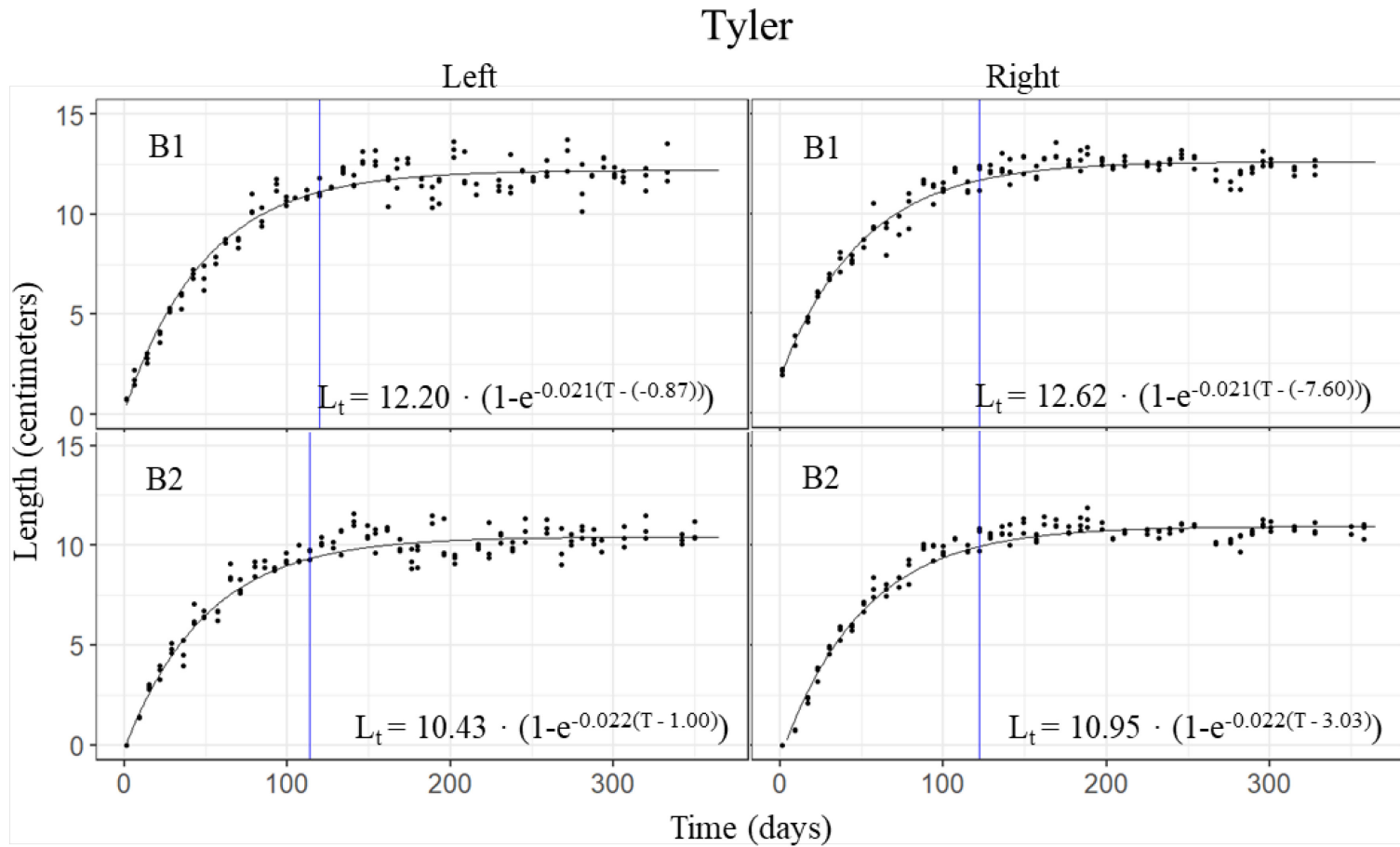
Figure 2-7E. von Bertalanffy equations fitted to the triplicate vibrissa length data for the two posterior macrovibrissae in row B for captive harp seal (*Pagophilus groenlandicus*), *Tyler.* von Bertalanffy equations are listed in the bottom right corner for each vibrissa. The blue vertical line represents the breakpoint when the vibrissa reached an asymptotic length.
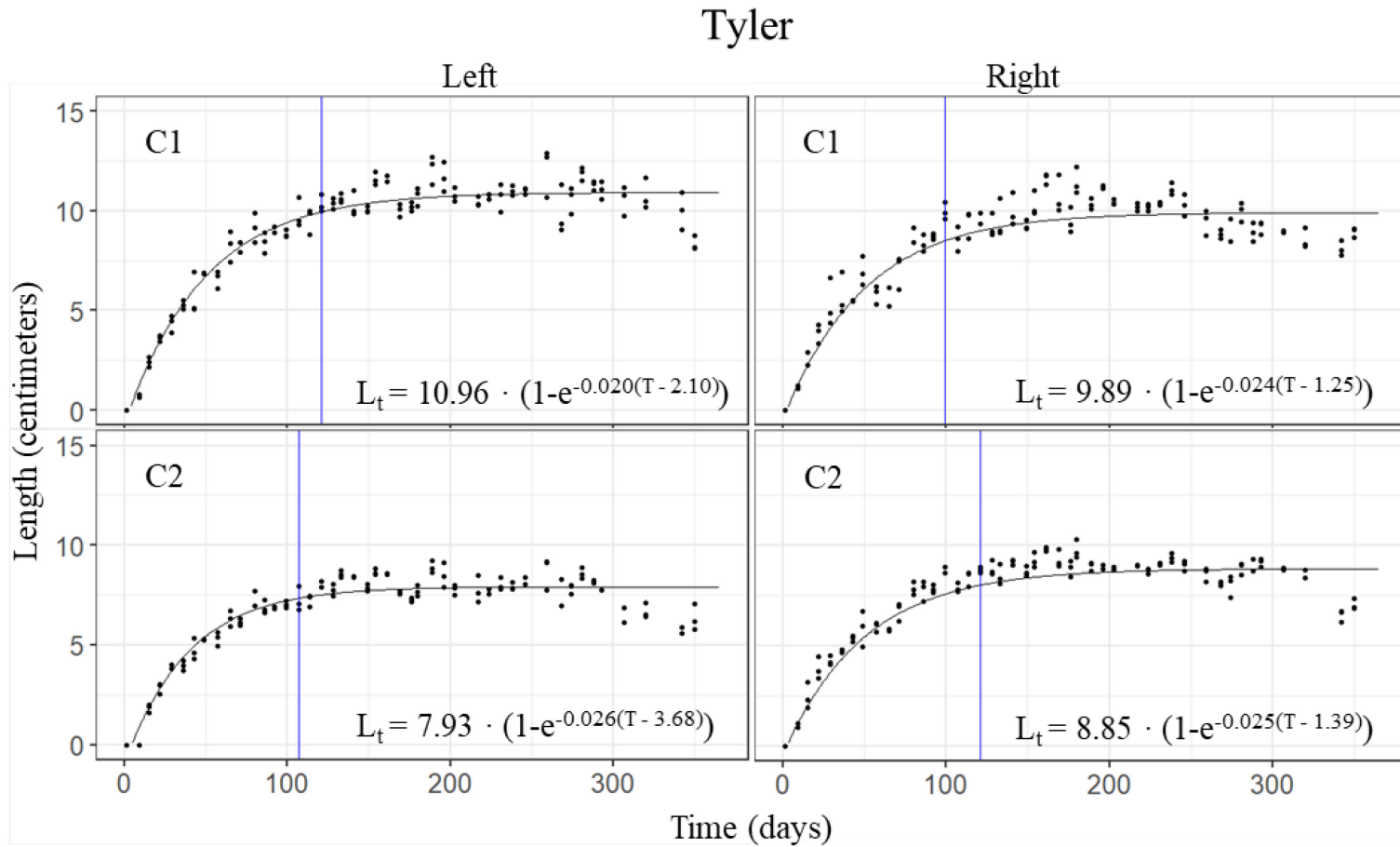
Figure 2-7F. von Bertalanffy equations fitted to the triplicate vibrissa length data for the two posterior macrovibrissae in row C for captive harp seal (*Pagophilus groenlandicus*), *Tyler.* von Bertalanffy equations are listed in the bottom right corner for each vibrissa. The blue vertical line represents the breakpoint when the vibrissa reached an asymptotic length.
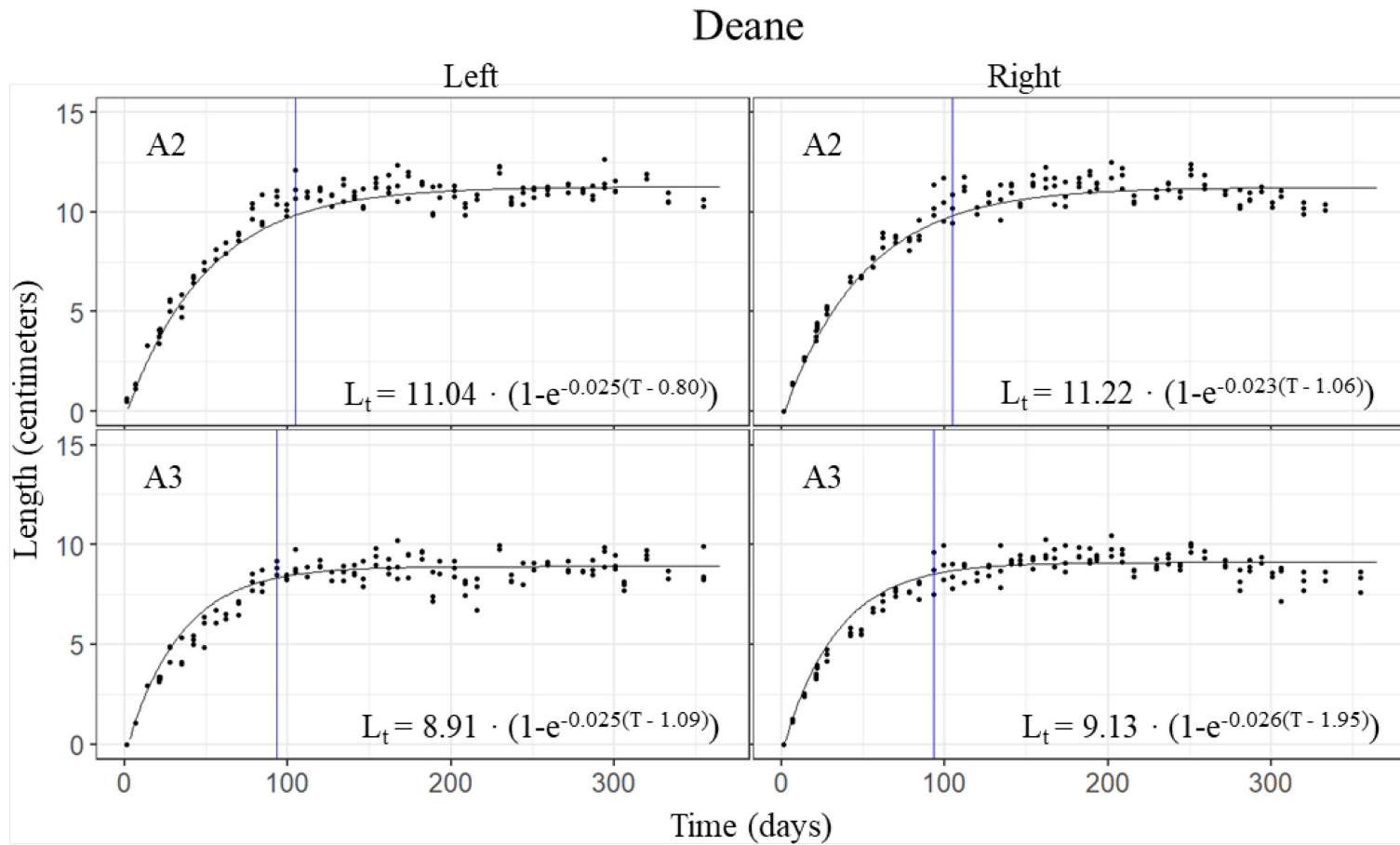
Figure 2-7G. von Bertalanffy equations fitted to the triplicate vibrissa length data for the two posterior macrovibrissae in row A for captive harp seal (*Pagophilus groenlandicus*)*, Deane*. von Bertalanffy equations are listed in the bottom right corner for each vibrissa. The blue vertical line represents the breakpoint when the vibrissa reached an asymptotic length.

Deane

Left — B1
$$L_t = 10.13 \cdot (1-e^{-0.032(T-2.93)})$$

Right — B1
$$L_t = 12.16 \cdot (1-e^{-0.020(T-4.14)})$$

Left — B2
$$L_t = 10.72 \cdot (1-e^{-0.024(T-2.77)})$$

Right — B2
$$L_t = 10.99 \cdot (1-e^{-0.022(T-2.75)})$$

Length (centimeters)

Time (days)
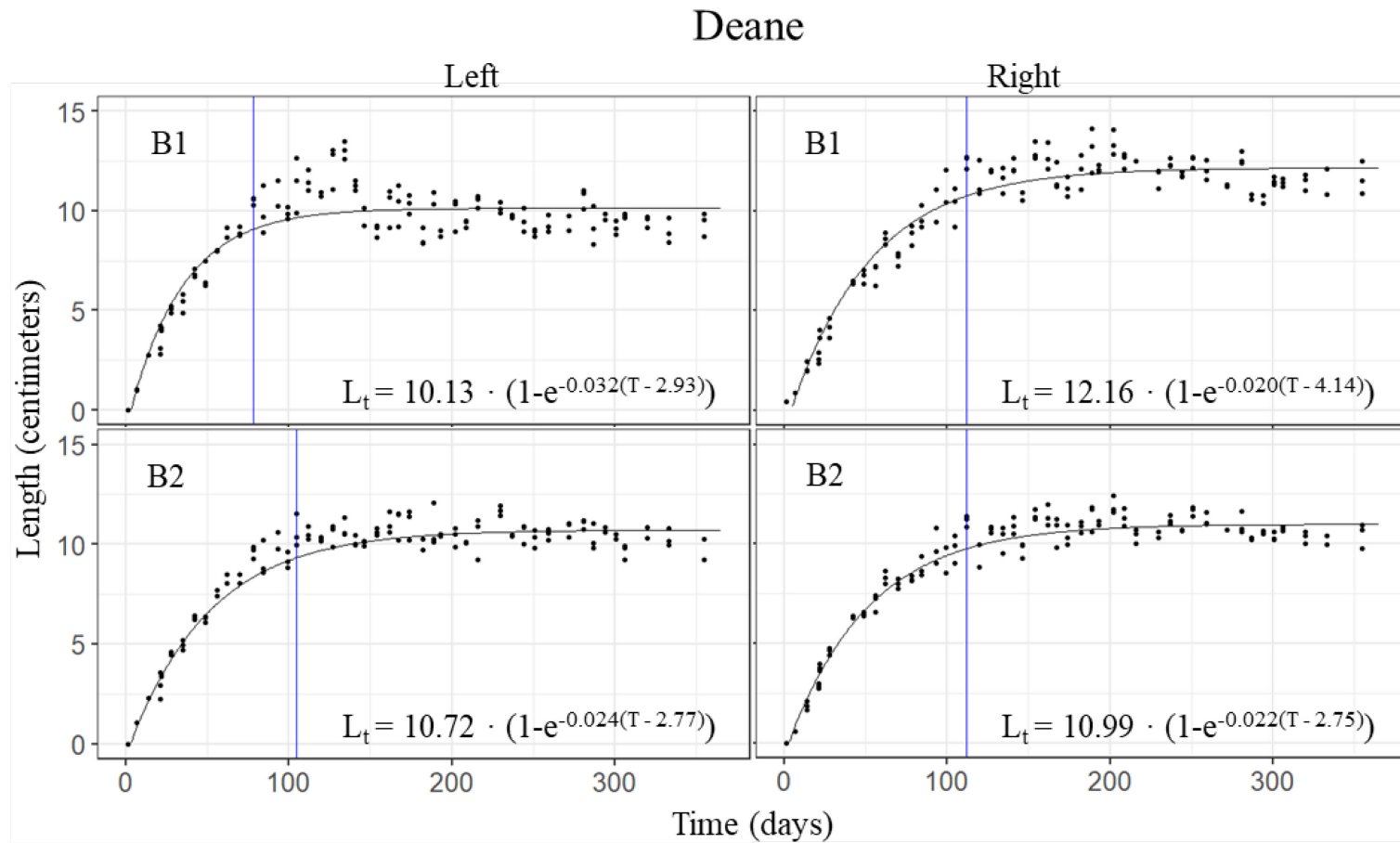
Figure 2-7H. von Bertalanffy equations fitted to the triplicate vibrissa length data for the two posterior macrovibrissae in row B for captive harp seal (*Pagophilus groenlandicus*)*, Deane.* von Bertalanffy equations are listed in the bottom right corner for each vibrissa. The blue vertical line represents the breakpoint when the vibrissa reached an asymptotic length.
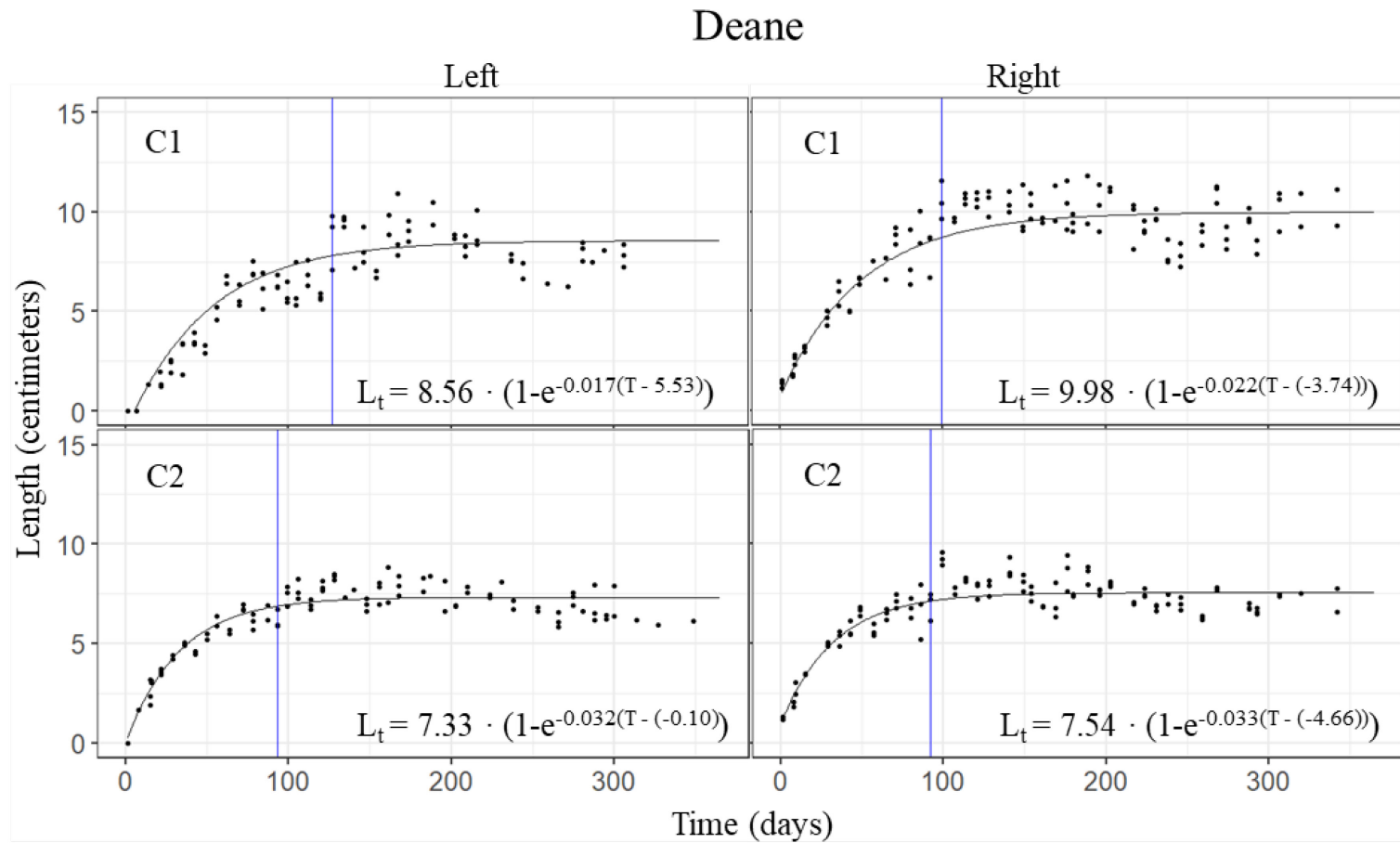
Figure 2-7I. von Bertalanffy equations fitted to the triplicate vibrissa length data for the two posterior macrovibrissae in row C for captive harp seal (*Pagophilus groenlandicus*), *Deane*. von Bertalanffy equations are listed in the bottom right corner for each vibrissa. The blue vertical line represents the breakpoint when the vibrissa reached an asymptotic length.
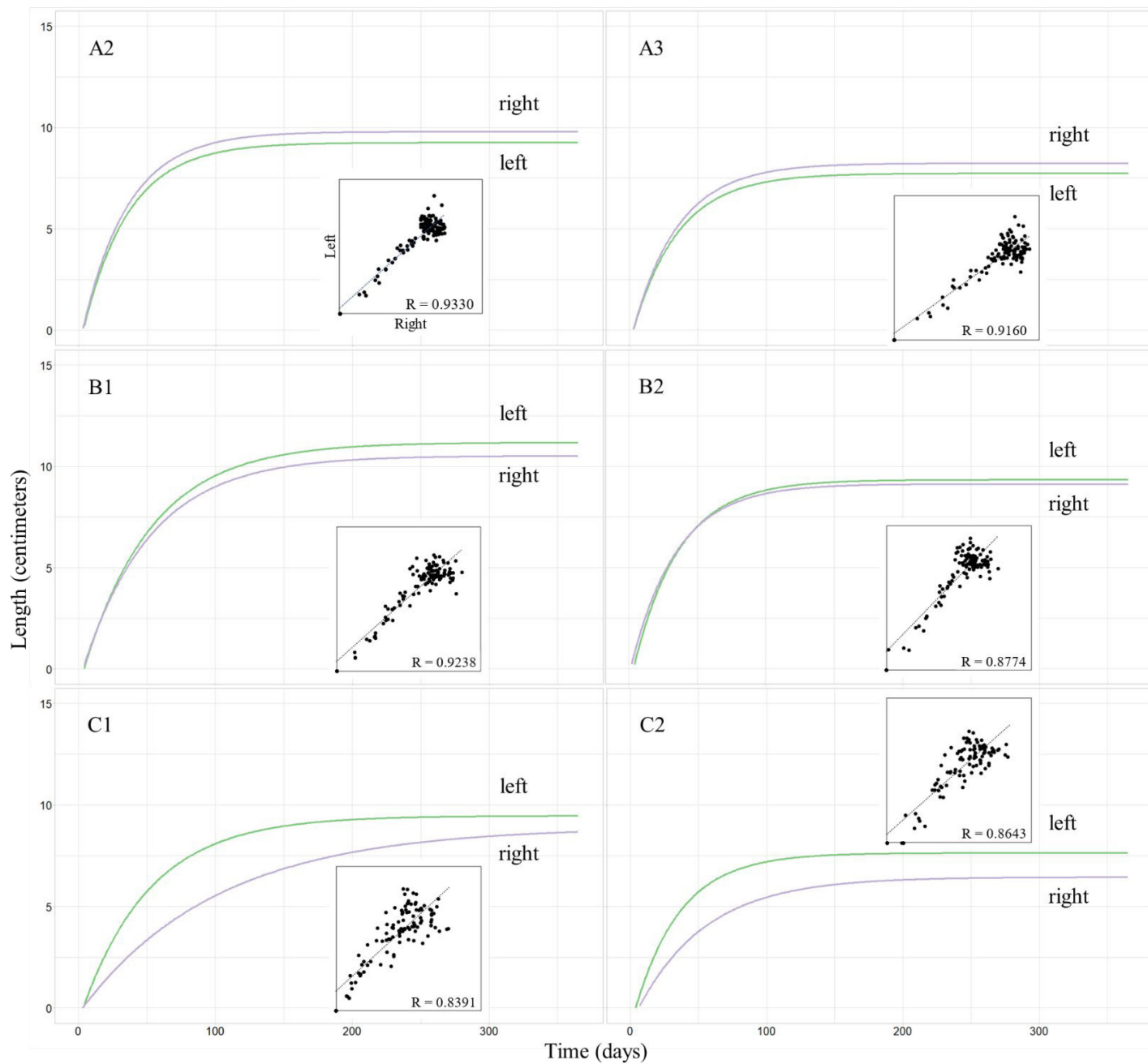
Figure 2-8A. von Bertalanffy growth equations plotted for captive harp seal (*Pagophilus groenlandicus), Babette*. The two posterior macrovibrissae in rows A, B, and C were compared on the left and right sides. The linear regression of the left versus right sides is inlaid in the plot with the coefficient of correlation.
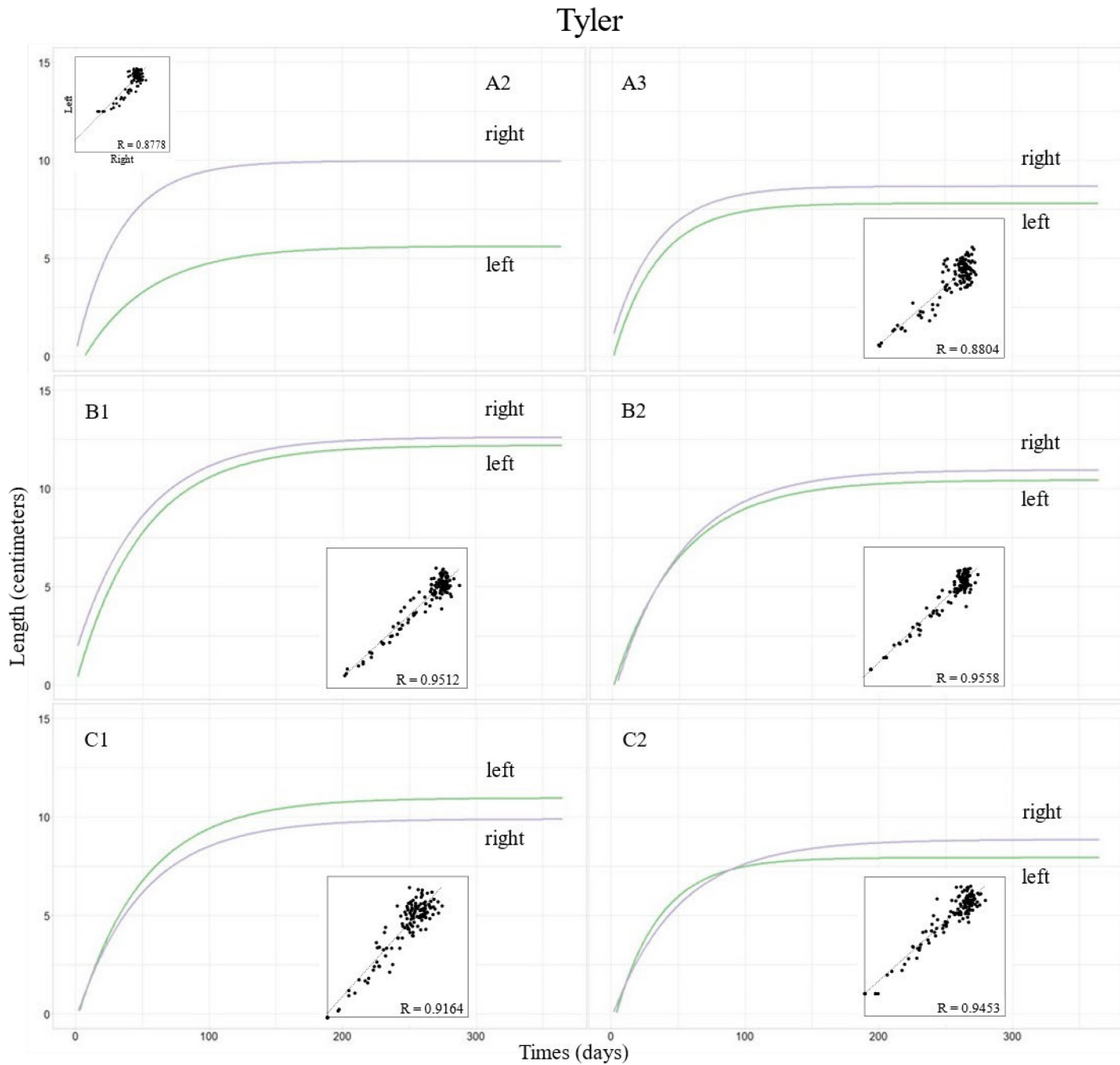
Figure 2-8B. von Bertalanffy growth equations plotted for captive harp seal (*Pagophilus groenlandicus), Tyler*. The two posterior macrovibrissae in rows A, B, and C were compared on the left and right sides. The linear regression of the left versus right sides is inlaid in the plot with the coefficient of correlation.
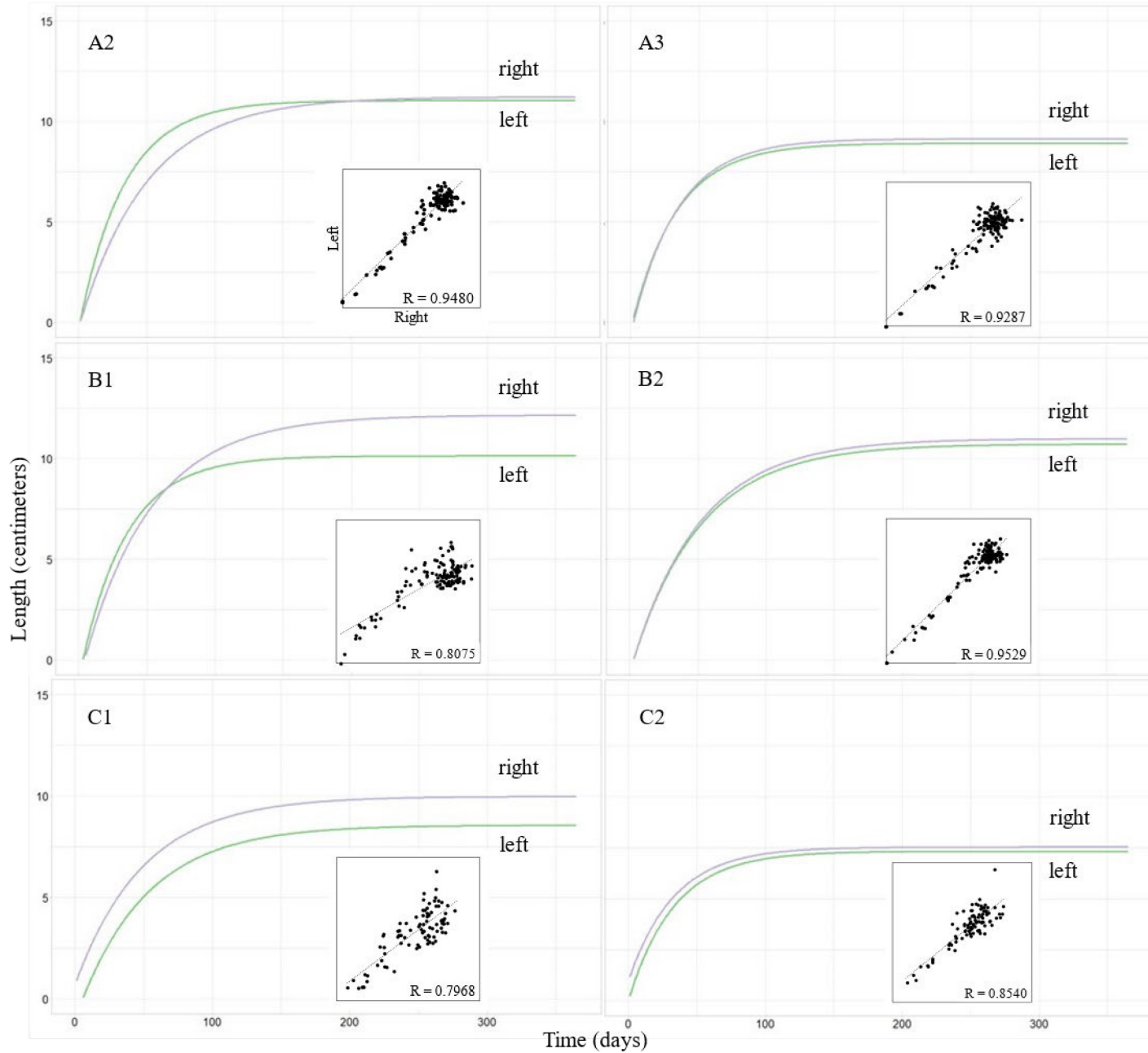
Figure 2-8C. von Bertalanffy equations fitted to vibrissa growth data are plotted for captive

harp seal (*Pagophilus groenlandicus), Deane*. The two posterior macrovibrissae in rows A, B,

and C were compared on the left and right sides. The linear regression of the left versus right

sides is inlaid in the plot with the coefficient of correlation.
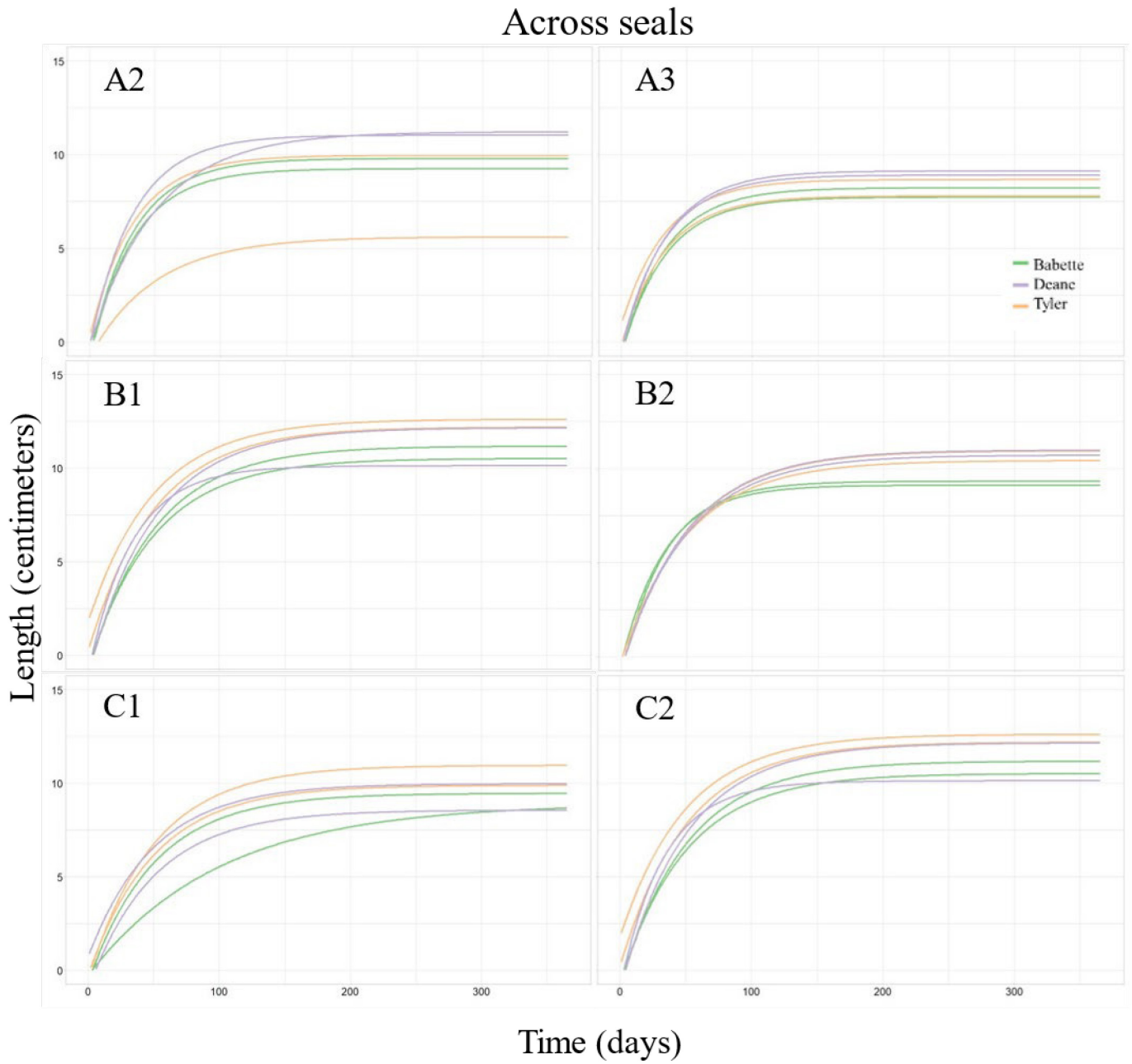
Figure 2-9. von Bertalanffy equations fitted to vibrissa growth data are plotted for captive harp seals (*Pagophilus groenlandicus), Babette, Tyler,* and *Deane*. The two posterior macrovibrissae in rows A, B, and C were compared across the three seals.
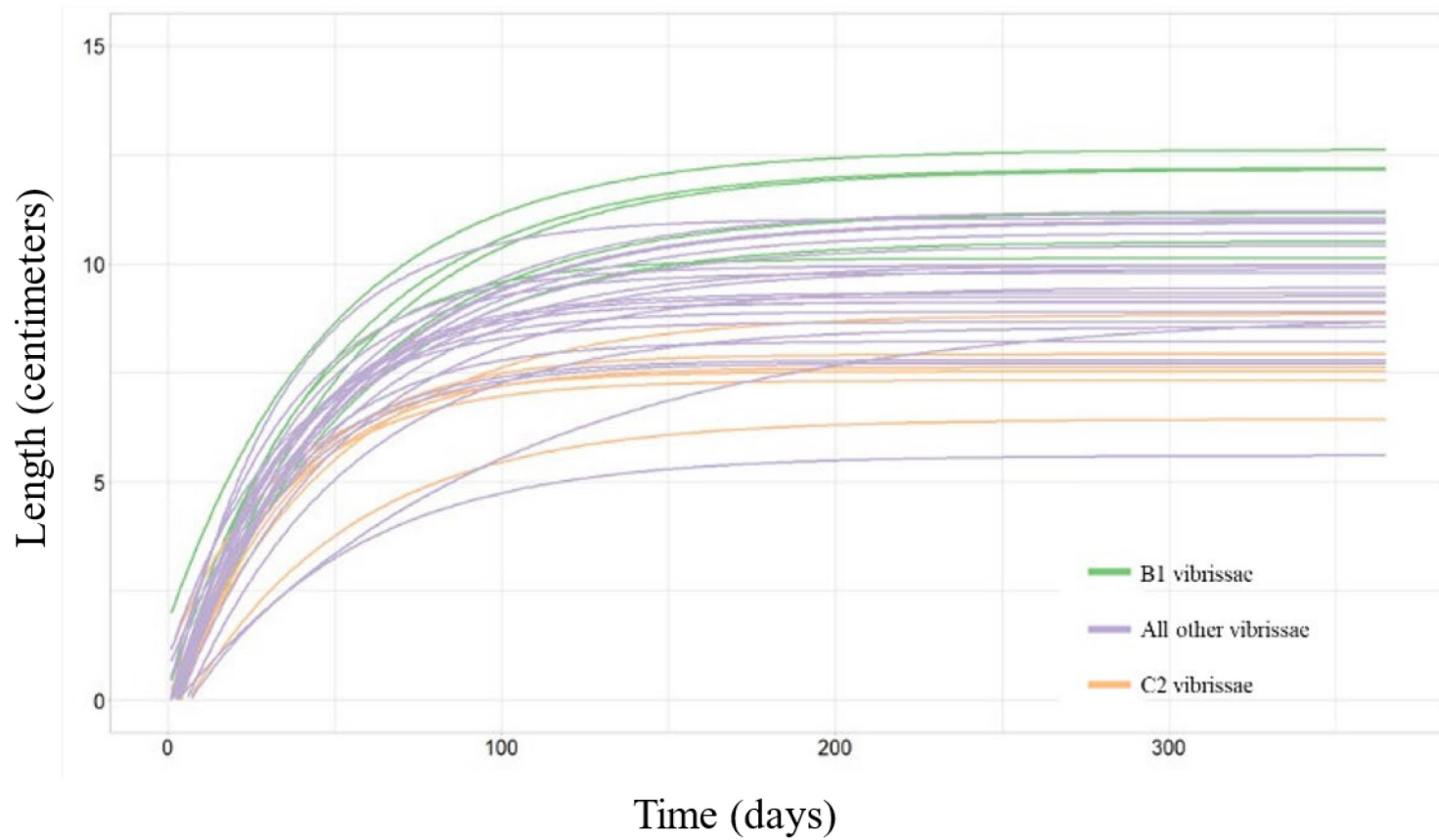
Figure 2-10. von Bertalanffy equations fitted to vibrissa growth data for the two posterior macrovibrissae of captive harp seals (*Pagophilus groenlandicus*) *Babette, Tyler,* and *Deane*. B1 vibrissae are coloured green, while C2 vibrissae are coloured orange. Vibrissae in positions A2, A3, B2, C1 are coloured purple.

Chapter 3 Summary, study limitations and conclusions

In summary, this study was the first to characterize the growth and shedding of captive harp seal vibrissae. Vibrissa growth was asymptotic, and shedding occurred synchronously, just prior to the moult of body pelage. The growth of vibrissae began at the end of March and ended in July or mid-August, depending on vibrissa position. The individual variations in vibrissa lengths prevented the use of the same von Bertalanffy parameter estimates across seals, which will create challenges for assigning a time of isotopic deposition to a position along the vibrissa. However, understanding the life events occurring during the period of vibrissa growth will provide researchers with valuable information for future ecological studies.

When sampling vibrissae from free-ranging seals, I would recommend sampling the vibrissa in the B1 position, as it is most often the longest vibrissa and easiest to identify. Whether the vibrissa is cut flush with the face or plucked, removing the root part of the vibrissa prior to analysis is recommended due to unexpected results from other non-keratinous tissue and blood attached to the root of the vibrissa (Karpovich et al., 2019). Depending on the study, vibrissa samples could be obtained from the annual harvest, post-mortem, or when animals are gathered in pupping areas prior to mating and moulting.

Vibrissae are a great candidate for measuring concentrations of environmental pollutants including mercury, trace elements, and persistent organic pollutants. Hormone concentrations can potentially be measured from mating season to implantation, and similarly, cortisol concentrations can be measured from mating, moulting, migration, and Arctic inhabitation. Analysis of stable isotopes can help researchers understand where the seals go after moulting, and what they are consuming, as they cross different isoscapes in the North Atlantic. Therefore, vibrissae are a useful, non-invasive method to study many ecological and physiological parameters in harp seals.

Future research considerations

Exploratory analysis should be completed on harp seal vibrissae to determine if useful ecological data can be extracted from vibrissae representing different life events including moulting, migration, and Arctic inhabitation. Stable isotopes, reproductive hormones, and environmental contaminants would be great candidates for exploratory analyses.

Future studies should investigate the lag period in deposition from when the seal consumes its prey to when the corresponding isotopes appear in the vibrissa. This would affect the interpretation of stable isotopes deposited during the moult when the seals feed minimally, and during periods of very fast vibrissa growth. This is also applicable to interpreting other ecological and physiological analyses. Researchers can study the lag period by giving the seals fluorescent markers in their food at a specific date and then measuring when the markers appear in the vibrissa. This could also help us understand how stored lipids are metabolized during the pelage moult, and the amount of time that occurs between prey consumption and appearance in the vibrissa. Depending on the length of the lag period and the timing of isotope deposition, the vibrissa could contain more data from the Arctic habitat.

Another consideration is the length of the vibrissa hidden subcutaneously. A calibration procedure for several pinniped species was developed to account for the length of vibrissa hidden subcutaneously (Sadou et al., 2014). The subcutaneous length varied by vibrissa position and was correlated with overall vibrissa length. These intradermal lengths would need to be measured for harp seals and considered if the vibrissa was plucked or a stray vibrissa was found on the ice.

A final future research suggestion would be to conduct a daily shedding study on the complete vibrissa profile of harp seals, which encompasses all micro- and macrovibrissae.

Although observations were made that most vibrissae were shed synchronously, this study was exclusive to the two exterior macrovibrissae of rows A, B, and C. Such a study could identify if all vibrissae are shed during the annual moult or if some are retained and shed at different periods. Asynchronous vibrissa shedding over the year would allow for different life events to be captured from over the annual cycle while retaining the seal's ability to forage for food. Complete vibrissa shedding while moulting is advantageous for the seal, as feeding is limited during this period, and all vibrissae would be replaced at one time.

Conclusions

In this year-long study, I obtained the first fine-scale measurements of vibrissa growth in captive harp seal vibrissae. I examined growth and shedding patterns in macrovibrissae and concluded that vibrissae followed a von Bertalanffy pattern of growth. Shedding occurred synchronously just prior to the annual pelage moult, with vibrissae shedding in March and April. A comparison of von Bertalanffy equations showed that parameter estimates were similar in some of the left and right positions within an individual seal. However, von Bertalanffy equations were different across seals and due to variations in vibrissa lengths, aging the vibrissae of free-ranging seals will be challenging. Vibrissae are a great candidate for future ecological studies, as long as researchers are able to work within the limitations of the asymptotic growth profile and variation in shedding dates of the vibrissae.

References

Alharbi, O. M., Khattab, R. A., & Ali, I. 2018. Health and environmental effects of persistent organic pollutants. *Journal of Molecular Liquids*, 263, 442-453.

Bauer, G., Reep, R., & Marshall, C. 2018. The tactile senses of marine mammals. *International Journal of Comparative Psychology,* 31, 1-28.

Bell, C. M., Hindell, M. A., & Burton, H. R. 1997. Estimation of body mass in the southern elephant seal, *Mirounga leonina*, by photogrammetry and morphometrics. *Marine Mammal Science*, 13, 669-682.

Beltran, R. S., Connolly Sadou, M., Condit, R., Peterson, S., Reichmuth, C., & Costa, D. P. 2015. Fine-scale whisker growth measurements can reveal temporal foraging patterns from stable isotope signatures. *Marine Ecology Progress Series,* 523, 243-253.

Bowen, W. D., & Iverson, S. J. 2013. Methods of estimating marine mammal diets: a review of validation experiments and sources of bias and uncertainty. *Marine Mammal Science*, 29, 719-754.

Brecht, M., Preilowski, B., & Merzenich, M. M. 1997. Functional architecture of the mystacial vibrissae. *Behavioural Brain Research,* 84, 81-97.

Cerrato, R. M. 1990. Interpretable statistical tests for growth comparisons using parameters in the von Bertalanffy equation. *Canadian Journal of Fisheries and Aquatic Sciences,* 47, 1416-1426.

Chabot, D., Stenson, G. B., & Cadigan, N. B. 1996. Short-and long-term fluctuations in the size and condition of harp seal (*Phoca groenlandica*) in the northwest Atlantic. *NAFO Scientific Council Studies*, 26, 15-32.

Cubillos, L. A. 2013. Fitting von Bertalanffy growth function. RPubs.

    https://rpubs.com/lacs/1123

Dauwe, T., Jaspers, V., Covaci, A., Schepens, P., & Eens, M. 2005. Feathers as a nondestructive

    biomonitor for persistent organic pollutants. *Environmental Toxicology and Chemistry:*

    An International Journal, 24, 442-449.

Dehnhardt, G. 1994. Tactile size discrimination by a California sea lion (*Zalophus californianus*)

    using its mystacial vibrissae. *Journal of Comparative Physiology A,* 175, 791-800.

Dehnhardt, G., Mauck, B., Hanke, W., & Bleckmann, H. 2001. Hydrodynamic trail-following in

    harbour seals (*Phoca vitulina*). *Science,* 293, 102-104.

Doi, H., Akamatsu, F., & González, A. L. 2017. Starvation effects on nitrogen and carbon stable

    isotopes of animals: an insight from meta-analysis of fasting experiments. *Royal Society Open*

    Science, 4, p.170633.

Driscoll, C. T., Mason, R. P., Chan, H. M., Jacob, D. J., & Pirrone, N. 2013. Mercury as a global

    pollutant: Sources, pathways, and effects. *Environmental Science and Technology,* 47,

    4967-4983

Eglite, E., Mohm, C., & Dierking, J. 2023. Stable isotope analysis in food web research:

    systematic review and a vision for the future for the Baltic Sea macro-region. *Ambio,* 52,

    319-338.

Espinasse, B., Sturbois, A., Basedow, S. L., Hélaouët, P., Johns, D. G., Newton, J., & Trueman,

    C. N. 2022. Temporal dynamics in zooplankton δ 13C and δ 15N isoscapes for the North

    Atlantic Ocean: Decadal cycles, seasonality, and implications for predator ecology.

    Frontiers in Ecology and Evolution, 10, 986082.

Gastaldi, A., Bishop, A., & Rea, L. D. 2023. How small can you go? Using a direct mercury analyzer to measure mercury in vibrissae of Steller sea lions. *Marine Mammal Science*, 39, 1005-1010.

Ginter, C. C., Fish, F. E., & Marshall, C. D. 2010. Morphological analysis of the bumpy profile of phocid vibrissae. *Marine Mammal Science*, 26, 733-743.

Greaves, D. K., Hammill, M. O., Eddington, J. D., Pettipas, D., & Schreer, J. F. 2004. Growth rate and shedding of vibrissae in the gray seal, *Halichoerus grypus*: a cautionary note for stable isotope diet analysis. *Marine Mammal Science,* 20, 296-304.

Grecian, W. J., Stenson, G. B., Biuw, M., Boehme, L., Folkow, L. P., Goulet, P. J., Jonsen, I. D., Malde, A., Nordøy, E. S., Rosing-Asvid, A. & Smout, S. 2022. Environmental drivers of population-level variation in the migratory and diving ontogeny of an Arctic top predator. *Royal Society Open Science*, 9, 211042.

Haley, M. P., Deutsch, C. J., & Le Boeuf, B. J. 1991. A method for estimating mass of large pinnipeds. *Marine Mammal Science*, 7, 157-164.

Hammill, M. O., Lesage, V., & Carter, P. 2005. What do harp seals eat? Comparing diet composition from different compartments of the digestive tract with diets estimated from stable-isotope ratios. *Canadian Journal of Zoology*, 83, 1365-1372.

Hirons, A. C., Schell, D. M., & St. Aubin, D. J. 2001. Growth rates of vibrissae of harbour seals (*Phoca vitulina*) and Steller sea lions (*Eumetopias jubatus*). *Canadian Journal of Zoology,* 79, 1053-1061.

Hobson, K. A., Schell, D. M., Renouf, D., & Noseworthy, E. 1996. Stable carbon and nitrogen isotopic fractionation between diet and tissues of captive seals: implications for dietary

reconstructions involving marine mammals. *Canadian Journal of Fisheries and Aquatic Sciences,* 53, 528-533.

Hobson, K. A., & Wassenaar, L. I. 2008. Tracking Animal Migration with Stable Isotopes. London, UK: *Academic Press*,

Hobson, K. A. 2023. Stable isotopes and a changing world. *Oecologia*. 203, 233-250.

Hurtado, S. I., Zaninelli, P. G., & Agosta, E. A. 2020. A multi-breakpoint methodology to detect changes in climatic time series. An application to wet season precipitation in subtropical Argentina. *Atmospheric Research*, 104955.

Jaishankar, M., Tseten T., Anbalagan, N., Mathew, B. B., & Beeregowda, K. N. 2014. Toxicity, mechanism and health effects of some heavy metals. *Interdisciplinary Toxicology* 7, 60-72.

Karpovich, S. A., Skinner, J. P., Kapronczai, L. A., Smith, J. A., & Janz, D. M. 2019. Examination of relationships between stable isotopes and cortisol concentrations along the length of phocid whiskers. *Marine Mammal Science*, 35, 395-415.

Karpovich, S. A., Horstmann, L. A., & Polasek, L. K. 2020. Validation of a novel method to create temporal records of hormone concentrations from the claws of ringed and bearded seals. *Conservation Physiology*, 8, p.coaa073.

Karpovich, S. A., Skinner, J. P., Miller, C. N., Polasek, L. K., & Pendleton, G. W. 2022. Growth and shedding of harbour seal (*Phoca vitulina*) whiskers. *Canadian Journal of Zoology,* 100, 687-699.

Kelley, K. W., Curtis, S. E., Marzan, G. T., Karara, H. M., & Anderson, C. R. 1973. Body surface area of female swine. *Journal of Animal Science*, 36, 927-930.

Keogh, M. J., Charapata, P., Fadely, B. S., Zeppelin, T., Rea, L., Waite, J. N., Burkanov, V., Marshall, C., Jones, A., Sprowls, C., & Wooller, M. J. 2021. Whiskers as a novel tissue for tracking reproductive and stress-related hormones in North Pacific otariid pinnipeds. *Conservation Physiology*. 9, coaa134.

Kershaw, J. L., & Hall, A. J. 2016. Seasonal variation in harbour seal (*Phoca vitulina*) blubber cortisol-A novel indicator of physiological state? *Scientific Reports*, 6, 21889.

Kernaleguen, L., Cazelles, B., Arnould, J. P., Richard, P., Guinet, C., & Cherel, Y. 2012. Long-term species, sexual and individual variations in foraging strategies of fur seals revealed by stable isotopes in whiskers. *PLoS One,* 7, e32916.

Kimura, D. 1980. Likelihood methods for the von Bertalanffy growth curve. *Fishery Bulletin,* 77, 765-776.

Kooyomjian, C., Giarikos, D., Adkesson, M., & Hirons, A. C., 2022. Evaluation of trace element concentrations in the serum and vibrissae of Peruvian pinnipeds (*Arctocephalus australis* and *Otaria byronia*). *The Journal of Wildlife Diseases*, 58, 608-620.

Kruger, Y., Hanke, W., Miersch, L., & Dehnhardt, G. 2018. Detection and direction discrimination of single vortex rings by harbour seals (*Phoca vitulina*). *Journal of Experimental Biology,* 221, jeb170753.

Lawson, J. W. & Stenson, G. B. 1997. Diet of Northwest Atlantic harp seals (*Pagophilus groenlandicus*) in offshore areas. *Canadian Journal of Zoology,* 75, 2095-2106.

Lesage, V., Hammill, M. O., & Kovacs, K. M. 2001. Marine mammals and the community structure of the Estuary and Gulf of St Lawrence, Canada: evidence from stable isotope analysis. *Marine ecology progress series*, 210, 203-221.

Ling, J. K. 1977. Vibrissae of marine mammals. In Functional Anatomy of Marine Mammals,

    Vol. 3 (ed. by J. B. Harrison), Academic Press, London, 387-415

Lowe, C. L., Hunt, K. E., Rogers, M. C., Neilson, J. L., Robbins, J., Gabriele, C. M., Teerlink, S.

    S., Seton, R., & Buck, C. L. 2021. Multi-year progesterone profiles during pregnancy in

    baleen of humpback whales (*Megaptera novaeangliae*). *Conservation Physiology*, 9,

    p.coab059.

Lübcker, N., Condit, R., Beltran, R. S., de Bruyn, P. J. N., & Bester, M. N. 2016. Vibrissa growth

    parameters of southern elephant seals (*Mirounga leonina*): obtaining fine-scale,

    time-based stable isotope data. *Marine Ecology Progress Series*, 559, 243-255.

Marshall, C. D., Amin, H., Kovacs, K. M., & Lydersen, C. 2006. Microstructure and innervation

    of the mystacial vibrissal follicle-sinus complex in bearded seals, *Erignathus barbatus*

    (Pinnipedia: Phocidae). *The Anatomical Record Part A: Discoveries in Molecular,*

    Cellular, and Evolutionary Biology: An Official Publication of the American Association

    of Anatomists, 288, 13-25.

Mattson, E. E., & Marshall, C. D. 2016. Follicle microstructure and innervation vary between

    pinniped micro- and macrovibrissae. *Brain Behaviour and Evolution,* 88, 43-58.

McHuron, E. A., Walcott, S. M., Zeligs, J., Skrovan, S., Costa, D. P., & Reichmuth, C. 2016.

    Whisker growth dynamics in two North Pacific pinnipeds: implications for determining

    foraging ecology from stable isotope analysis. *Marine Ecology Progress Series,* 554,

    213-224.

McHuron, E. A., Holser, R. R., & Costa, D. P. 2018. What's in a whisker? Disentangling

    ecological and physiological isotopic signals. *Rapid Communications Mass Spectrometry,*

    33, 57-66.

McHuron, E. A., Williams, T., Costa, D. P., & Reichmuth, C. 2020. Contrasting whisker growth dynamics within the phocid lineage. *Marine Ecology Progress Series,* 634, 231-236.

Miller, E. H. 1975. A comparative study of facial expressions of two species of pinnipeds. *Behaviour,* 53, 268–284.

Miller, E. H., & Kochnev, A. A. 2021. Ethology and behavioral ecology of the walrus (*Odobenus rosmarus*), with emphasis on communication and social behavior. In *Ethology and behavioral ecology of otariids and the odobenid.* 437-488. Cham: Springer International Publishing.

Minagawa, M., Wada, E. 1984. Stepwise enrichment of 15N along food chains: further evidence and the relation between d15N and animal age. *Geochimica Cosmochimica Acta,* 48, 1135-1140.

Nelson, G. A. 2021. Package 'fishmethods' fishery science methods and models. R package version 1.12-1. CRAN. CRAN.R-project.org/package=fishmethods

Ortiz, R. M., Houser, D. S., Wade, C. E., & Ortiz, C. L. 2003. Hormonal changes associated with the transition between nursing and natural fasting in northern elephant seals (*Mirounga angustirostris*). *General and Comparative Endocrinology,* 130, 78-83.

Page, H. M. 1997. Importance of vascular plant and algal production to macro-invertebrate consumers in a southern California salt marsh. *Estuarine, Coastal and Shelf Science,* 45, 823-834

Pettitt, A. N. 1979. A Non-Parametric Approach to the Change-Point Problem. *Journal of the Royal Statistical Society.* 28,126-135.

R Core Team. 2021. R: A language and environment for statistical computing. R Foundation for Statistical Computing. https://www.R-project.org/

Ramsay, M. A., Hobson, K. A. 1991 Polar bears make little use of terrestrial food webs: evidence from stable-carbon isotope analysis. *Oecologia* 86, 598-600.

Rea, L. D., Christ, A. M., Hayden, A. B., Stegall, V. K., Farley, S. D., Stricker, C. A., Mellish, J.-A. E., Maniscalco, J. M., Waite, J. N., Burkanov, V. N., & Pitcher, K. W. 2015. Age-specific vibrissae growth rates: a tool for determining the timing of ecologically important events in Steller sea lions. *Marine Mammal Science,* 31, 1213-1233.

Rea, L. D., Castellini, J. M., Avery, J. P., Fadely, B. S., Burkanov, V. N., Rehberg, M. J., & O'Hara, T. M. 2020. Regional variations and drivers of mercury and selenium concentrations in Steller sea lions. *Science of the Total Environment*, 744, 140787.

Rosing-Asvid, A. 2008. A new harp seal whelping ground near south Greenland. *Marine Mammal Science*, 24, 730-736.

Sadou, M. 2014. Short note: a calibration procedure for measuring pinniped vibrissae using photogrammetry. *Aquatic Mammals,* 40, 213-218.

Sanvito, S., Galimberti, F., & Miller, E. H. 2007. Having a big nose: structure, ontogeny, and function of the elephant seal proboscis. *Canadian Journal of Zoology*, 85. 207-220.

Schneider, C. A., Rasband, W. S., & Eliceiri, K. W. 2012. NIH Image to ImageJ: 25 years of image analysis. *Nature Methods,* 9, 671-675.

Sergeant, D. 1991. Harp seals, man and ice. *Canadian Special Publication of Fisheries and Aquatic Sciences,* 114, 1-153.

Sergeant, D. 1965. Migrations of harp seals *Pagophilus groenlandicus* in the Northwest Atlantic. *Journal of the Fisheries Research Board of Canada,* 22, 433-464.

Shatz, L. F., & De Groot, T. 2013. The frequency response of the vibrissae of harp seal, *Pagophilus groenlandicus*, to sound in air and water. *PLoS One,* 8, e54876.

Smith, R. J., Hobson, K. A., Koopman, H. N., Lavigne, D. M. 1996. Distinguishing between

populations of fresh- and saltwater harbour seals (*Phoca vitulina*) using stable-isotope

ratios and fatty acid profiles. *Canadian Journal of Fisheries and Aquatic Sciences*, 53,

272-279.

Smodlaka, H., Galex, I., Palmer, L., Borovac, J. A., & Khamas, W. A. 2017. Ultrastructural,

sensory, and functional anatomy of the northern elephant seal (*Mirounga angustirostris*)

facial vibrissae. *Anatomia Histologia, Embryologia,* 46, 487-496.

Stenson, G. B., Haug, T., & Hammill, M. O. 2020. Harp seals: monitors of change in differing

ecosystems. *Frontiers in Marine Science,* 7, 569258.

Stenson, G. B., Buren, A. D., & Koen-Alonso, M. 2016. The impact of changing climate and

abundance on reproduction in an ice-dependent species, the Northwest Atlantic harp seal,

Pagophilus groenlandicus. *ICES Journal of Marine Science,* 73, 250-262.

Stenson, G. B., & Hammill, M. O. 2014. Can ice breeding seals adapt to habitat loss in a time of

climate change? *ICES Journal of Marine Science,* 71, 1977-1986.

Stenson, G. B., & Sjare, B. 1997. Seasonal distribution of harp seals, *Phoca groenlandica*, in the

Northwest Atlantic. *ICES Council Meeting Papers*. 23.

Stenson, G. B., Rivest, L. P., Hammill, M. O., & Gosselin, J. F. 2003. Estimating pup production

of harp seals, *Pagophilus groenlandicus*, in the Northwest Atlantic. *Marine Mammal

Science,* 19, 141-60.

von Ehrenstein, O. S., Guha Mazumder, D. N., Hira-Smith, M., Ghosh, N., Yuan, Y., Windham,

G., Ghosh, A., Haque, R., & Lahiri, S. 2006. Pregnancy outcomes, infant mortality, and

arsenic in drinking water in West Bengal, India. *American Journal of Epidemiology* 163,

662-669.

Williams, C., & Kramer, E. M. 2010. The advantages of a tapered whisker. *PloS One*, 5, e8806.

Wieskotten, S., Mauck, B., Miersch, L., Dehnhardt, G., & Hanke, W. 2011. Hydrodynamic discrimination of wakes caused by objects of different size or shape in a harbour seal (*Phoca vitulina*). *Journal of Experimental Biology*, 214, 1922-1930.

Wilson, K., Littnan, C., Halpin, P., & Read, A. 2017. Integrating multiple technologies to understand the foraging behaviour of Hawaiian monk seals. *Royal Society Open Science*, 4, 160703.

Yablokov, A. V., & Klevezal, G. A.1962 (1969). Whiskers of whales and seals and their distribution, structure, and significance. In: *Morphological Characteristics of Aquatic Mammals* (S.E. Kleinenberg, Ed.) (in Russian). Nauka, Moscow, USSR. Fisheries Research Board of Canada Translation Series No. 1335, 48-41.

Zhao, L., & Schell, D. M. 2004. Stable isotope ratios in harbour seal *Phoca vitulina* vibrissae: effects of growth patterns on ecological records. *Marine Ecology Progress Series,* 281, 267-273.

Appendices

Appendix A

Hypotheses for the likelihood-ratio tests to compare von Bertalanffy growth equations among and across seals.

H$_o$: von Bertalanffy parameter estimates are equal,

H$_1$: Asymptotic-lengths (L$_\infty$) parameter estimates are not equal,

H$_2$: K growth-coefficient parameter estimates are not equal,

H$_3$: Time-of-initial-growth (T$_o$) parameter estimates are not equal,

H$_4$: All von Bertalanffy parameter estimates are not equal.

Within seal comparisons:

The null (H$_o$) and alternative (H$_a$) hypotheses of the likelihood ratio tests were set up as follows:

Alternative hypothesis 1 (H$_1$) Asymptotic lengths:

H$_o$: L$_\infty$LV$_x$ = L$_\infty$RV$_x$,

H$_1$: L$_\infty$LV$_x \neq$ L$_\infty$RV$_x$,

Where L$_\infty$LV$_x$ is the parameter estimate of the asymptotic length for vibrissa x on the left side, and L$_\infty$RV$_x$ is the parameter estimate of the asymptotic length of vibrissa x on the right side.

Alternative hypothesis 2 (H$_2$) K growth constants:

H$_o$: KLV$_x$ = KRV$_x$,

H$_2$: KLV$_x \neq$ KRV$_x$.

Where KLV_x is the parameter estimate of the growth constant for vibrissa x on the left side, and KRV_x is the parameter estimate of the growth constant of vibrissa x on the right side.

Alternative hypothesis 3 (H_3) The initial time of growth:

H_o: $T_o LV_x = T_o RV_x$,

H_3: $T_o LV_x \neq T_o RV_x$

Where $T_o LV_x$ is the parameter estimate of the initial time of growth for the vibrissa on the left side, and T_oRV_x is the parameter estimate of the time of initial growth of the vibrissa on the right side.

Alternative hypothesis 4 (H_4) all von Bertalanffy parameters:

H_o: $L_\infty LV_x + KLVx + T_oLV_x = L_\infty RV_x + KRV_x + T_oRV_x$,

H_4: $L_\infty LV_x + KLVx + T_oLV_x \neq L_\infty RV_x + KRV_x + T_oRV_x$,

The null hypothesis states that all parameter estimates in the von Bertalanffy model on the left and right side of the face are equal for vibrissa x, and the alternative hypothesis states that all the parameter estimates are not equal.

Across seal comparisons:

Alternative hypothesis 1 (H_1) asymptotic lengths:

H_o: $L_\infty BLV_x = L_\infty TLV_x = L_\infty DLV_x = L_\infty BRV_x = L_\infty TRV_x = L_\infty DRV_x$,

H_1: $L_\infty BLV_x \neq L_\infty TLV_x \neq L_\infty DLV_x \neq L_\infty BRV_x \neq L_\infty TRV_x \neq L_\infty DRV_x$,

Where $L_\infty BLV_x$ and $L_\infty BRV_x$ are the parameter estimates of the asymptotic length for *Babette*'s

vibrissa x on the left and right sides, respectively. $L_\infty TLV_x$ and $L_\infty TRV_x$ are the parameter

estimates of the asymptotic length of the vibrissa x on the left and right sides of *Tyler*'s face.

Lastly, $L_\infty DLV_x$ and $L_\infty DRV_x$ are the parameter estimates of the asymptotic length of *Deane*'s

vibrissa x on the left and right sides.

Alternative hypothesis 2 (H_2) K growth constants:

H_o: $KBLV_x = KTLV_x = KDLV_x = KBRV_x = KTRV_x = KDRV_x$,

H_2: $KBLV_x \neq KTLV_x \neq KDLV_x \neq KBLV_x \neq KTLV_x \neq KDLV_x$.

Where $KBLV_x$ is the parameter estimate of the growth constant for *Babette*'s vibrissa x on the

left side. Similarly, $KTLV_x$ is the parameter estimate of the growth constant of the vibrissa x on

the left side of *Tyler*'s face. $KDLV_x$ is the estimate of the growth constant of *Deane*'s left

vibrissa x.

Alternative hypothesis 3 (H_3) the initial time of growth:

H_o: $T_o BLV_x = T_o TLV_x = T_o DLV_x = T_o BRV_x = T_o TRV_x = T_o DRV_x$,

H_3: $T_o BLV_x \neq T_o TLV_x \neq T_o DLV_x \neq T_o BRV_x \neq T_o TRV_x \neq T_o DRV_x$

Where $T_o BLV_x$ and $T_o BRV_x$ are the parameter estimates of the time of initial growth for

Babette's vibrissae x on the left and right sides. Similarly, $T_o TLV_x$ is the parameter estimate of

the time of initial growth of the x vibrissa on the left side of *Tyler*'s face. $T_o DLV_x$ is the estimate

of the time of initial growth of *Deane*'s left vibrissa x, and $T_o DRV_x$ is the for the right side.

Alternative hypothesis 4 (H_4) all von Bertalanffy parameter estimates:

H_o: $L_\infty BLV_x = L_\infty TLV_x = L_\infty DLV_x = L_\infty BRV_x = L_\infty TRV_x = L_\infty DRV_x$, $KBLV_x = KTLV_x = KDLV_x = KBRV_x = KTRV_x = KDRV_x$, $T_oBLV_x = T_oTLV_x = T_oDLV_x = T_oBRV_x = T_oTRV_x = T_oDRV_x$,

H_4: $L_\infty BLV_x \neq L_\infty TLV_x \neq L_\infty DLV_x \neq L_\infty BRV_x \neq L_\infty TRV_x \neq L_\infty DRA2$, $KBLV_x \neq KTLV_x \neq KDLV_x \neq KBRV_x \neq KTRV_x \neq KDRV_x$, $T_oBLV_x \neq T_oTLV_x \neq T_oDLV_x \neq T_oBRV_x \neq T_oTRV_x \neq T_oDRV_x$,

Similar to the previous hypotheses, the first letter represents the parameter estimate, the second letter represents the seal, the third letter represents the side of the face, and V_x represents the alphanumeric position of the vibrissa. The null hypothesis is set up as all parameter estimates being equal for the three seals, and the alternative hypothesis has all the parameter estimates not equal.